Geomorphology 418 (2022) 108462

Contents lists available at ScienceDirect

Geomorphology

journal homepage: www.journals.elsevier.com/geomorphology

Spatio-temporal differences dominate suspended sediment dynamics in medium-sized catchments in central Germany

Jan Henrik Blöthe [a,*], Thomas Hoffmann [b]

[a] Institute of Environmental Social Sciences and Geography, University of Freiburg, Schreiberstraße 20, 79085 Freiburg, Germany
[b] Federal Institute of Hydrology, Am Mainzer Tor 1, 56068 Koblenz, Germany

ARTICLE INFO

Keywords:
Suspended sediment transport
Specific sediment yield
Hydrograph separation
Hysteresis
Extreme events
German upland rivers

ABSTRACT

Suspended sediment transport, dominating material export from lowland river systems, is highly variable in space and time. Since suspended sediment transport can have adverse effects on human infrastructure, targeted management is imperative. To achieve this, a thorough understanding of suspended sediment dynamics is needed, but requires long-term monitoring data. Despite studies investigating suspended sediment dynamics on decadal time scales, an assessment of the spatio-temporal variability across adjacent river catchments is still lacking.

To fill this gap, we analyse suspended sediment transport at twelve stations along German upland rivers, monitored on a daily basis for 28 to 54 years. All monitoring stations belong to the Rhine (Lahn, Lippe, Main, and Neckar) and Weser river systems (Fulda, Leine, Werra, and Weser) and have contributing areas between 2500 and 22,000 km^2. Although located in comparable topo-climatic settings, average sediment yield for the monitoring period varied more than fourfold. Covering the range of 5.9 to 28.7 t km^{-2} yr^{-1}, we found the highest and lowest suspended sediment yields for the Neckar and Lippe catchments, respectively. Using two different streamflow separation approaches, we estimated the contribution of stormflow discharge to total sediment transport to fall between 73 and 85 % in the Neckar and Lahn rivers while remaining ~15 % lower for the remaining catchments. Investigating the relevance of extreme events, we found the share of total suspended sediment load transported during the ten largest events to vary between ~28 % for the Neckar and ~8 % for the Lippe and Werra catchments. These events were predominantly characterized by clockwise hysteresis loops that hint to in-channel reworking as a significant material source, with the exception of the Neckar stations where anti-clockwise hysteresis patterns prevailed. Here, the hysteresis analysis indicates sediment delivery from more distant sources in the headwater regions, likely related to elevated rainfall intensities and the susceptibility of the escarpment of the Swabian Alb towards landsliding. We conclude that the combined effect of varying rainfall amounts and intensities, the fraction of steeper slopes as well as lithological differences explain the across-catchment variability on multiple time scales that is further modulated by river management practices.

1. Introduction

Suspended sediment transport is considered the dominant mode of material transfer from continents to oceans (Walling and Fang, 2003) and plays a fundamental role for the geomorphic evolution of lowland river systems (Owens et al., 2005). At the same time, suspended sediment is a vector for both nutrients and contaminants and is therefore of vital ecological importance (Frings et al., 2014; Naden, 2010; Vanmaercke et al., 2011). Extreme events, likely becoming more frequent in future, have the potential to dramatically alter channel morphology and by that leave a sustained impact on river ecosystems (Death et al., 2015). From a natural hazards perspective, adverse effects of sediment erosion, suspended transport and deposition further include river bed degradation, damage to infrastructure, loss of reservoir capacity, and the siltation of estuaries and coastal waters (Vanmaercke et al., 2011; Vercruysse et al., 2017). A thorough quantification and understanding of suspended sediment loads in central European river systems is therefore urgently needed to assess the geomorphic and ecological impacts of changing environmental conditions, as well as for natural hazard mitigation, sediment management and improving the surface water quality in the

* Corresponding author.
E-mail address: jan.bloethe@geographie.uni-freiburg.de (J.H. Blöthe).

https://doi.org/10.1016/j.geomorph.2022.108462
Received 6 May 2022; Received in revised form 12 August 2022; Accepted 19 September 2022
Available online 21 September 2022

context of the European Water Framework directive.

The concentration of suspended sediments measured in the river at a certain place and time depends on the complex interaction of geomorphological and hydro-meteorological processes, combined with the influence of human alterations to natural systems. Anthropogenic modifications within river catchments can impact sediment dynamics in many ways (see Wohl, 2015 for a comprehensive review). Most prominently, changes in land-use and land-cover induce increased soil erosion and enhance sediment supply to the river system, while the construction of barriers within the channel interrupt longitudinal sediment connectivity and trap sediments, reducing overall sediment transfer (Belletti et al., 2020; Naden, 2010; Walling, 2006; Wohl, 2015).

While on a global scale differences in sediment loads from large rivers are primarily controlled by catchment area, climate and relief (Syvitski and Milliman, 2007), a European assessment also finds considerable variability within topo-climatic regions, pointing to additional factors gaining importance on the regional scale (Vanmaercke et al., 2011). Analysis of long-term (decadal to centennial) suspended sediment loads might provide further insight into internal processes operating within the catchment, as well as highlighting the effect of climate change on sediment and water flows in natural systems (Vercruysse et al., 2017). Since the propensity for intermittent sediment storage increases with catchment size (Hoffmann et al., 2013), sediment yield per unit area tends to decline with contributing area (Walling, 1983). This effect has been demonstrated in many studies, though a global analysis of >3000 records also points to the large scatter of sediment yield over three orders of magnitude for catchment sizes between 10^0 and 10^4 km^2 (García-Ruiz et al., 2015). In addition to contributing area, the number of records in the time series influence estimates on long-term annual sediment loads and the contribution of extreme events (Gonzalez-Hidalgo et al., 2010). Based on a meta-analysis of over 2500 records, García-Ruiz et al. (2015) conclude that reliable estimates require time-series in exceedance of 20 years, while pointing to the scarcity of studies covering >25 years on record at the same time. This is especially important, as robust monitoring studies can provide valuable insight into suspended sediment dynamics, but need to cover sufficiently long observation periods to encompass extreme events.

Yet monitoring networks of long-term sediment loads of entire river systems are still rare (Naden, 2010), until now limiting our understanding of the spatio-temporal variability of (suspended) sediment dynamics and its underlying causes. This is of particular relevance as suspended sediment transport is highly episodic: during floods, large quantities of suspended sediment are transported, whereas rivers at low-flows can be virtually free of sediments in suspension (Hoffmann et al., 2020). Despite numerous studies investigating suspended sediment dynamics, the authors are not aware of work addressing this relative contribution of stormflow and baseflow, i.e. the share of streamflow fuelled by groundwater or other delayed components (Hall, 1968), to total sediment transport in multiple adjacent river catchments. Yet whether the bulk sediment load is preferentially exported during events or during phases of low-flow influences the behaviour of hydro-geomorphic systems (Owens et al., 2005; Naden, 2010). Long-term monitoring of suspended sediment transport in multiple catchments is therefore crucial for a targeted sediment management.

For example, Oeurng et al. (2010) investigated the relevance of flood events for sediment transport in a ~1000 km^2 catchment in southern France, observing 95 % of annual sediment transport happened in 20 % of the time. However, their data is only spanning two years of continuous monitoring. On longer time-scales, Sun et al. (2016) studied the importance of flood events for suspended sediment transport in the ~5000 km^2 Loushui river catchment, China, and concluded that floods were responsible for an average 78 % of annual sediment transport from 1966 to 1985. For a second period, after the construction of a large reservoir in the catchment, this number reduced to ~55 % for the period from 2007 to 2011, highlighting the buffering effect of anthropogenic constructions on sediment dynamics (Sun et al., 2016). In conjunction with the relevance of extreme events, earlier studies investigating suspended sediment transport in Europe reported high intra-annual and inter-annual variability as well as distinct seasonal patterns (Harlow et al., 2006; Oeurng et al., 2010; Vercruysse et al., 2020).

In the absence of continuous high-resolution (minutes to days) measurements of suspended sediment, different techniques such as rating curves or linear interpolation are applied to estimate suspended sediment concentration from discharge data (Hoffmann et al., 2020; Warrick, 2015). While these techniques constitute important tools, estimated loads often show large variability depending on the frequency of data sampling and the respective methods used (Asselman, 2000; Skarbøvik et al., 2012; Walling and Webb, 1981). In this sense, an in-depth investigation of the spatio-temporal variability of suspended sediment transport in decadal time-series can help to better understand and ultimately predict sediment dynamics in a given catchment.

So far, comparative studies investigating the spatial variability of suspended sediment transport in multiple catchments over decadal time scales are rare, as the majority of studies investigating suspended sediment transport in medium sized catchments focus on the detailed investigation of single river systems (Oeurng et al., 2010; Vercruysse et al., 2020). But also on the scale of single river systems, spatial variability between individual tributaries can be immense. Ten years of monitoring suspended sediment yield for three tributaries of the Exe river in the UK (Harlow et al., 2006) revealed factor two differences in average specific sediment yield (SSY). Moreover, meta-studies of compiled data sets that investigated large scale spatial patterns in sediment dynamics found pronounced regional differences in (suspended) sediment transport (García-Ruiz et al., 2015; Vanmaercke et al., 2011), raising the question of regional variability and its underlying controls.

To address this shortcoming, we present an analysis of suspended sediment transport from twelve monitoring stations along six different river systems that span up to five decades of daily observations – to our knowledge the most comprehensive data set on modern sediment flux from European upland rivers. We specifically limit our study to rivers draining the German upland regions and hypothesize that minor differences in topo-climatic settings and catchment characteristics introduce significant spatio-temporal variability of sediment transport on multiple time scales in these neighbouring systems that range from 10^3 to 10^4 km^2.

Our objectives are i) to investigate the spatio-temporal variability of suspended sediment transport on multiple time scales (long-term, inter-annual, intra-annual, event), and ii) to quantify the relative contribution of baseflow and stormflow discharges as well as the contribution of the largest suspended sediment transport events (SSTE) to the total sediment transport.

2. Study area

To achieve this goal, we analysed suspended sediment concentration (SSC) and load (SSL) recorded at twelve monitoring stations along rivers draining the upland regions of Central Germany. All rivers drain towards the North Sea and belong to the Rhine (Lahn, Lippe, Main, and Neckar) and Weser (Fulda, Leine, Werra, and Weser) drainage systems, respectively (Fig. 1). Upstream contributing area ranges between 2589 and 21,501 km^2 (Table 1). At first glance, eleven of the twelve catchments have similar topographic settings, maximum elevation largely remains below 1000 m and the local relief of the catchments varies between ~780 and ~930 m. With a maximum elevation of ~620 m and a local relief of only ~560 m, the smallest catchment surveyed here, located at the Lippe river upstream of the monitoring station Hamm (HAL), is characterized by much gentler hillslope gradients. The 95th percentile of slope gradients remains below 9° here, while varying between ~14° and ~20° for the other stations (Table 1, Fig. S1).

Mean annual precipitation (MAP) as calculated from regionalized

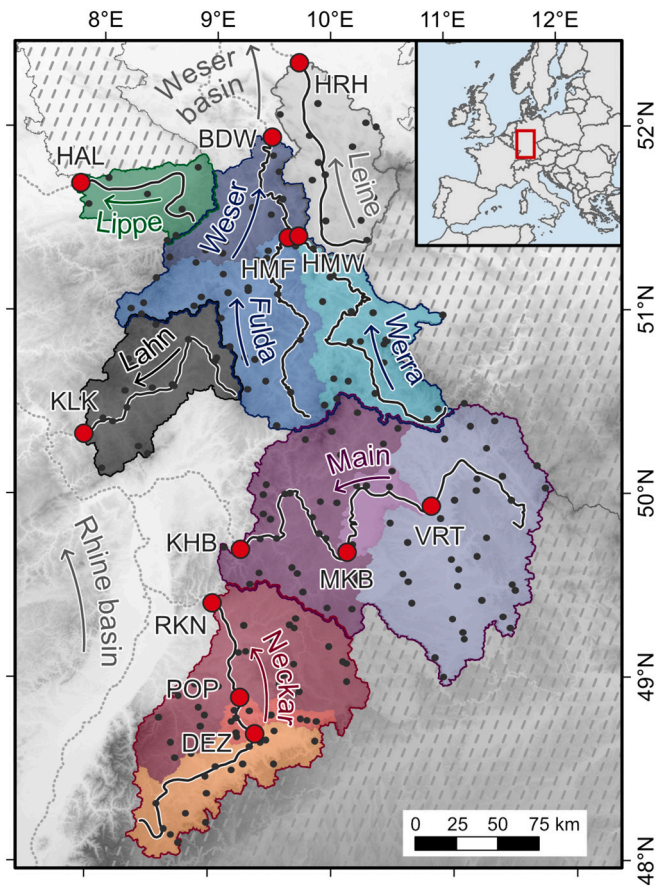

Fig. 1. Major rivers and their catchments in the German upland regions. Red dots show the location of monitoring stations for suspended sediment concentration surveyed in this study along with abbreviated names (Table 1). Small black dots indicate the location of weather stations. Blue, purple and red colour shadings show nested catchments of the Weser, Main and Neckar rivers, respectively, grey, green and black shading depict Leine, Lippe and Lahn catchments, respectively. Arrows show drainage direction of rivers, hatched area marks river systems that are not included in the analysis.

station data (DWD (Deutscher Wetterdienst) Climate Data Center (CDC), 2020a, 2020b) range between ~780 to ~950 mm, with large inter-annual variability (Table 1, Fig. S2). Within the catchments, orographic effects introduce distinct spatial differences with higher MAP in uplands and lower MAP in low lands. This pattern is modulated by a large-scale declining trend of MAP from western to eastern Germany. The runoff regime of all rivers surveyed in this study can be characterized as either pluvial (Rhine tributaries) or pluvial-nival (Weser tributaries) with low-flows occurring in late summer (August and September) and high-flows occurring in late winter (February and March) (Bormann, 2010). This regime pattern can be modulated by high-intensity precipitation events from convective cells predominantly occurring during the summer months.

It is important to note here that Central German waterways are heavily managed river systems. Erosion protection measures such as retaining walls and riverbank rip-rap run along most of the river reaches and limit channel migration. Along large parts of the surveyed waterways, barrages of several meters height guarantee navigability, but reduce flow variability and sediment dynamics at the same time. Upstream of the stations along the Leine and Lippe rivers, as well as the uppermost station on the Neckar and Main rivers, only one (HRH, VRT, and DEZ) or two (HAL) major barrages are located along the trunk river. The remaining river sections along the Neckar (POP 9 barrages, RKN 21 barrages), Main (MKB 11 barrages, KHB 24 barrages), Weser (BDW 14 barrages, HMF 9 barrages, HMW 5 barrages) and Lahn (KLK 16 barrages) are much more regulated, based on data available from the Federal Water and Shipping Administration (WSV (Wasserstraßen- und Schifffahrtsverwaltung des Bundes), 2022). Apart from in-channel barrages along federal waterways, the inventory of dams in Germany (Speckhann et al., 2021) locates 100 dams in the catchments surveyed here. In addition to these large scale constructions, Central European river systems are strongly fragmented by hundreds of thousands small-scale in-channel barriers that reduce longitudinal sediment connectivity (Belletti et al., 2020).

In terms of land use, determined here on the basis of EU Corine Land Cover data for 1990 (EEA (European Environment Agency), 2020a), all catchments are predominated by agricultural areas that occupy flat valleys and gently inclined plateaus of Central Germany, constituting between 49.0 and 58.5 % of the land cover, again with the exception of the Lippe catchment (74.0 %). Forests dominate the steeper hillslopes and cover between 33.5 and 43.8 % of the land surface (Lippe catchment 18.2 %). Interestingly, the catchments differ markedly in the percentage of artificially sealed surfaces such as roads and buildings that attain values from 9.5 to 13.0 % in the Neckar catchment, while remaining between 5.2 and 7.6 % for the other river systems.

The geology of the study area is predominated by Mesozoic sedimentary rocks, apart from Cenozoic volcanic rocks at the Vogelsberg, Röhn, and Westerwald in the Lahn, Fulda, and Werra catchments. The Lahn catchment can be considered an exception in this regard, as Devonian and Carboniferous sandstones and siltstones of the Rhenish Shield are more common here. The Mesozoic sedimentary units in the Weser and Leine catchments are predominated by Triassic sandstones and limestones, but also mudstones and marlstones are common. Parts of the Leine catchment drain the southwestern and western part of the Harz mountains that are characterized by sedimentary rocks from the Carboniferous, such as greywacke, sandstone and claystones. The Lippe hosts the youngest Mesozoic sedimentary rocks with marlstones, limestones and sandstones from the Cretaceous. Only at the south-eastern tip, metamorphosed quartzite and greywacke of the Rhenish Shield are exposed. The cuesta landscapes of the Swabian and Franconian Alb and their forelands, drained mainly by the Neckar and Main river systems in the southern part of Germany, are dominated by Mesozoic sedimentary rocks that are shallowly inclined in south-eastern direction. Here, the sedimentary successions vary in age from the middle Triassic to the youngest Cretaceous and are dominated by limestones and claystones (Henningsen and Katzung, 2011; Meschede, 2018). The resistant Jurassic limestones that build up the escarpments of the Swabian and Franconian Alb are often underlain by weak claystones, making the region prone to landsliding (Bell, 2007). In general, bedrock outcrops are very limited and most of the study area is covered by regolith and/or sedimentary cover. Sandwiched between the Fennoscandian and Alpine ice-sheets during the Pleistocene, the German upland regions host extensive loess deposits, covering between 9 and 37 % of the catchments surveyed here (Table 1) (Haase et al., 2007).

3. Methods

3.1. Suspended sediment data

Suspended sediment concentration (SSC) in German inland waterways has been monitored on a daily basis by the Federal Waterways and Shipping Administration at ~70 sampling locations, with first stations in operation since 1964. The twelve stations analysed here span various time intervals (Table 2), but each station covers at least 28 years of continuous monitoring. Monitoring intervals between stations have a minimum overlap of 25 years (between 1977 and 2002). At each monitoring site, daily 5-l water samples were filtered using commercial coffee filters, which were weighed before and after filtering in dry conditions to calculate the daily SSC (kg m^{-3}) (Hillebrand, 2013; Hoffmann et al., 2020). The application of coffee filters is of sufficient quality and cost-efficient, allowing for measurement of SSC at a large

Table 1
Selected monitoring stations and their associated catchment characteristics (see Fig. 1 for location).

Station name	Station name abbreviation	ID[a]	River	Basin area (km^2)[b]	Min elevation (m)[b]	Max elevation (m)[2]	95th percentile slope (°)[b]	Mean annual precipitation (mm)[c]	Corine Land Cover (% catchment area)[d]				Loess cover[f] (% catchment area)
									Artificial surface[e]	Agricultural areas[e]	Forest and seminatural areas[e]	Wetlands and water bodies[e]	
Deizisau	DEZ	220	Neckar	3,995	241	1023	19.75	953	10.3	53.2	36.4	0.0	9.0
Poppenweiler	POP	221	Neckar	4,969	202	1023	18.85	920	13.0	52.1	34.8	0.1	11.6
Rockenau	RKN	222	Neckar	12,673	130	1023	17.52	894	9.5	54.4	36.0	0.1	23.6
Viereth	VRT	231	Main	11,981	228	1043	14.56	797	5.9	54.0	40.0	0.2	10.8
Marktbreit	MKB	232	Main	13,480	180	1043	14.31	785	6.0	55.4	38.4	0.3	14.6
Kleinheubach	KHB	233	Main	21,501	122	1043	15.07	784	5.2	55.7	38.8	0.3	20.5
Kalkofen	KLK	241	Lahn	5,306	69	879	15.76	792	7.2	49.0	43.7	0.1	22.1
Hamm	HAL	277	Lippe	2,589	53	616	8.98	855	7.5	74.0	18.2	0.3	37.3
Hann.-Münden	HMW	401	Werra	5,500	118	988	18.29	791	5.1	51.0	43.8	0.2	11.3
Hann.-Münden	HMF	402	Fulda	6,945	120	948	16.30	788	5.6	50.4	43.7	0.3	22.1
Bodenwerder	BDW	403	Weser	15,943	63	988	17.16	799	5.2	51.8	42.9	0.2	15.9
Herrenhausen	HRH	421	Leine	5,313	49	929	15.89	810	7.6	58.5	33.5	0.4	31.2

[a] Station IDs from 220 to 277 belong to the Rhine drainage system, station IDs from 401 to 421 belong to the Weser drainage system.
[b] As determined from EU-DEM v1.1 (25 × 25 m) © European Union, Copernicus Land Monitoring Service 2020, European Environment Agency (EEA).
[c] Calculated from daily REGNIE rainfall data provided by the German weather service (DWD (Deutscher Wetterdienst) Climate Data Center (CDC), 2020a, 2020b, see Rauthe et al., 2013 for processing details).
[d] Taken from Corine Land Cover 1990 version 2020 © European Union, Copernicus Land Monitoring Service 2020, European Environment Agency (EEA).
[e] Artificial surfaces include classes 1.1.1 to 1.4.2; Agricultural areas include classes 2.1.1. to 2.4.4.; Forest and seminatural areas include classes 3.1.1. to 3.3.5.; Wetlands and water bodies include classes 4.1.1. to 5.1.2.
[f] Loess cover after European Loess Map (Haase et al., 2007).

number of stations. During floods the sampling frequency was increased to three samples per day, unless sampling was prohibited due to safety reasons. Sample processing does not separate mineral and organic fractions and therefore represents the concentration of the total suspended solids (Hoffmann et al., 2020). The suspended sediment mainly contained clay and silt and only a small fraction of fine sands, on average remaining below ~10 % for the Rhine river system (Frings et al., 2019).

As opposed to continuous automatic discharge measurements, SSC samples were taken manually since the beginning of measurements in 1964, restricting SSC data coverage to working days. To fill data gaps resulting from weekends, public holidays and technical difficulties, we estimated sediment rating curves for individual stations and scaled missing SSC values in our data. At many stations, there is a distinct break in the sediment rating relationship, with different rating domains above and below this break (Hoffmann et al., 2020). We therefore applied a lowess regression approach to compute the sediment rating relationships and scaled missing SSC values from daily mean discharge (Q) (Cleveland, 1979; Hoffmann et al., 2020). On average, data gaps in SSC affected ~115–130 days (~30–35 %) per year.

Monitoring intervals of the twelve stations range between 28 and 54 complete years (Table 2), resulting in a total of 192,485 SSC values. From these monitoring data we derived daily, monthly, annual as well as long-term, SSL (given in t yr^{-1}) and SSY (given in t km^{-2} yr^{-1}). SSL and SSY were calculated by the sum of daily loads (kg day^{-1}) that we derived from daily data on SSC (kg m^{-3}) and Q (m^3 s^{-1}) as measured at the monitoring sites and the fixed network of gauging stations, respectively. While discharge is monitored at or close to most SSC monitoring sites, for three stations (HAL, MKB, POP) we relied on more distant gauging stations. However, it was assured that no major tributaries enter between SSC monitoring sites and gauging stations. Long-term averaged SSL and SSY presented in this study cover the full monitoring interval of each station. Since monitoring periods vary in length and only partially overlap, long-term average SSL and SSY between stations may differ due to long-term trends and year-to-year variability.

3.2. Hydrograph separation

To better understand suspended sediment dynamics, it is imperative to assess whether the bulk of SSL is exported during events of high-flows (stormflow), or whether a significant fraction is retained and exported during subsequent non-event discharge (baseflow). In the absence of comprehensive data on baseflow and stormflow contributions to total discharge, we relied on modelling flow components from discharge data to estimate the proportion of sediment load transported during different stages. A wide range of approaches exist to separate total runoff into baseflow and stormflow components. We acknowledge here that despite underlying physical reasoning, hydrograph separation techniques are essentially arbitrary, as the model output is a conceptual value and not a physical property (Nathan and McMahon, 1990; Pelletier and Andréassian, 2020). However, the conceptual idea of different flow components offers a way to quantify the proportion of sediment load transported during short-lived events and during longer-lasting non-event discharge.

Here we used two different approaches for hydrograph separation. First, we applied the Lyne and Hollick (1979) approach that uses a recursive filter on discharge time-series for hydrograph separation. Though the approach itself is straightforward, the specific application and parameter definition varies. Here we followed the guidelines proposed for a standard application of the filter by Ladson et al. (2013), and implemented in the R package *hydrostats* (www.r-project.org). For all stations, we set the number of passes to three (for daily data) and used a value of 0.975 for the filter parameter *a*, which influences the attenuation of the event hydrograph.

Second, we separated the streamflow following Pelletier and Andréassian (2020) that conceptualize baseflow as the output from a reservoir. Acting as the catchment's discharge memory, the reservoir

Table 2
Discharge, specific suspended sediment yield (SSY) and annual suspended sediment load (SSL) for selected monitoring stations (see Fig. 1 for location).

Station name	Station name abbreviation	ID	River	Basin area (km^2)[a]	Discharge ($m^3\ s^{-1}$)			SSY ($t\ km^{-2}\ yr^{-1}$)			SSL ($kt\ yr^{-1}$)			Observation period	
					LQ	MQ	HQ	Min	Mean	Max	Min	Mean	Max	Start-end	Years
Deizisau	DEZ	220	Neckar	3,995	8	52	1031	4.55	27.18	77.21	18.17	108.60	308.46	1975–2002	28
Poppenweiler	POP	221	Neckar	4,969	6	63	1288	4.29	28.65	184.78	21.29	142.37	918.18	1966–2013	48
Rockenau	RKN	222	Neckar	12,673	18	137	2140	5.24	25.92	83.10	66.46	328.44	1053.17	1972–2018	47
Viereth	VRT	231	Main	11,981	14	107	1270	2.07	6.75	14.99	24.82	80.92	179.64	1973–2005	33
Marktbreit	MKB	232	Main	13,480	13	113	1180	3.56	9.54	23.99	47.97	128.55	323.39	1966–2011	46
Kleinheubach	KHB	233	Main	21,501	11	172	1720	2.97	10.49	26.14	63.96	225.49	562.05	1974–2010	37
Kalkofen	KLK	241	Lahn	5,306	3	44	759	2.84	11.35	34.87	15.08	60.22	185.01	1971–2018	48
Hamm	HAL	277	Lippe	2,589	4	24	203	1.65	5.85	19.04	4.26	15.15	49.29	1977–2017	41
Hann.-Münden	HMW	401	Werra	5,500	9	50	425	6.88	16.67	47.11	37.81	91.69	259.10	1966–2018	53
Hann.-Münden	HMF	402	Fulda	6,945	8	63	720	2.20	8.93	23.95	15.28	62.02	166.35	1966–2018	53
Bodenwerder	BDW	403	Weser	15,943	30	148	1190	3.88	11.02	34.85	61.87	175.61	555.65	1965–2018	54
Herrenhausen	HRH	421	Leine	5,313	10	52	799	5.19	19.05	64.67	27.56	101.20	343.61	1966–2004	39

[a] As determined from EU-DEM v1.1 (25 × 25 m) © European Union, Copernicus Land Monitoring Service 2020, European Environment Agency (EEA).

receives input from the streamflow and releases water following a quadratic outflow function. Though computationally more demanding, the main advantage of this approach lies in the automated estimation of its parameter values, i) the reservoir capacity and ii) the hydro-climatic response time of the catchment. The functions to estimate these parameters from observed discharge and modelled effective precipitation data for the surveyed catchment are implemented in the R-Package *baseflow* (see details in Pelletier and Andréassian (2020)). For the estimation of effective precipitation, we relied on meteorological data from the station network of the German Weather Service (DWD (Deutscher Wetterdienst) Climate Data Center (CDC), 2021). In total, we used 223 weather stations within the catchment boundaries that have a minimum overlap of five years with the observation periods of the monitoring stations (Fig. 1, Table S1). For each station, we computed daily mean air temperatures for all climate stations located within the catchment boundaries and derived a daily temperature lapse rate using a linear model. We then scaled daily mean temperatures to the mean elevation of the river catchment to derive potential evapotranspiration following Oudin et al. (2005). Using the Turc-Mezentsev formula, we then calculated effective precipitation from daily precipitation and modelled potential evapotranspiration (Mezentsev, 1955; Pelletier and Andréassian, 2020; Turc, 1954).

From both hydrograph separation approaches, we calculated stormflow indices (SFI) for all catchments, representing the share of total discharge attained during high-flow situations. Furthermore, we derived the daily, monthly, annual and long-term share of SSL and SSY transported during these high-flows by summing the daily stormflow contribution to SSL and SSY.

3.3. Identification of sediment load peaks and hysteresis classification

In addition to quantifying the relative contribution of baseflow and stormflow for suspended sediment transport, we investigated the amount of sediment exported during the largest suspended sediment transport events (SSTE). For this, we used a peak over threshold approach (e.g. Lang et al., 1999) to extract all events exceeding the 95th percentile of daily SSL at each station using the function 'event_detection_context' (R package *seriesdist*; https://rforge.net/seriesdist/svn.html). From these events, we selected the n-largest ($n = 2 \times$ observation period) SSTE, resulting in a data series with twice as many events as observation years for the individual stations. To ensure event independence, the function allows for the definition of a minimum gap that separates individual peaks. We modelled this minimum gap from observed sediment load data at all twelve stations following Skaugen and Onof (2014) and find speed of recession after peak values to fall between 3 and 5 days for our catchments.

To investigate hysteresis effects in the events identified above, we computed a hysteresis index (HI) that is based on the ratio of the SSC along the rising limb (SSC_{RL}) and SSC along the falling limb (SSC_{FL}) of a flood hydrograph. Given the daily data used in our study, we favoured a simple approach that compares SSC_{RL} and SSC_{FL} at the half range discharge between Q_{max} and Q_{min} for each event (Lawler et al., 2006) over more detailed quantification at multiple discharges (e.g. Lloyd et al., 2016). For clockwise hysteresis ($SSC_{RL} > SSC_{FL}$), HI was computed by:

$$HI = (SSC_{RL}/SSC_{FL}) - 1, \quad (1)$$

and for anti-clockwise hysteresis ($SSC_{RL} < SSC_{FL}$), HI was determined using:

$$HI = (-1/(SSC_{RL}/SSC_{FL})) + 1. \quad (2)$$

While the HI attains positive values for clockwise hysteresis and negative values for anti-clockwise hysteresis, the absolute value of the index is a proxy for the "fatness" (i.e. area) of the hysteresis loop (Lawler et al., 2006). Following the same basic idea, we further classified hysteresis patterns by computing the area of hysteresis loops, normalized by the maximum SSC and Q for each event, yielding negative surface areas for anti-clockwise hysteresis and positive surface areas for clockwise hysteresis. Both approaches are only capable of distinguishing three hysteresis types, i.e. clockwise, anti-clockwise and complex or straight.

3.4. Datasets for catchment characterisation

To investigate potential controls on the spatio-temporal patterns of suspended sediment transport we used a number of data sets that offered continuous and/or harmonized data covering each studied river catchment. For all topographic calculations, we relied on digital topographic data with 25 m ground resolution provided within the Copernicus framework of the European Union (EEA (European Environment Agency), 2020b). Furthermore, we used Corine Land Cover data with 100 m spatial ground resolution (EEA (European Environment Agency), 2020a) to derive land cover information for the catchments investigated here. We decided to use the Corine Land Cover data for the year 1990, as this falls in the centre of the common observation period of all stations. Though included in the Corine Land Cover data set, the Copernicus Land Monitoring Service also offers a higher resolution data set on impervious surfaces that gives the fraction of sealed surfaces within cells of 20 m ground resolution (EEA (European Environment Agency), 2020c). Furthermore, we used the European Loess Map (Haase et al., 2007) to assess the potential influence of easily erodible aeolian deposits on long-term sediment load. For precipitation, we used daily and monthly REGNIE (regionalised precipitation) data sets provided by the German weather service (DWD (Deutscher Wetterdienst) Climate Data Center

(CDC), 2020a, 2020b), a gridded spatially interpolated data set with a ground resolution of 1 × 1 km available from 1931 to present (Rauthe et al., 2013). We used REGNIE data to calculate daily, monthly, annual and mean annual precipitation (MAP) statistics for catchment boundaries derived from digital topographic data. To characterise extreme precipitation events in daily data, we used a threshold of 20 mm day^{-1} (Deumlich and Gericke, 2020) that roughly corresponds to the 99th percentile of daily catchment averaged precipitation in our data. Only for the estimation of potential evapotranspiration and effective precipitation, we used station data from the German Weather Service as described in Section 3.2. Finally, we draw on the mean annual rainfall erosivity product (Ballabio et al., 2017) that uses station data on rainfall energy and volume to estimate the erosive power of precipitation events.

4. Results

4.1. Spatial pattern of long-term sediment transport

The average long-term SSY, defined here as the mean of the observation period, at all twelve stations along German upland rivers varied by factor four between 5.9 and 28.7 t km^{-2} yr^{-1} (Table 2). Despite the topographic similarities of catchments draining the upland regions of Central Germany, mean and median long-term SSY increased significantly with MAP, the mean annual rainfall erosivity (Ballabio et al., 2017), the fraction of area covered by impervious surfaces, and the fraction of area with slopes steeper than 20° (Fig. 2). In turn, we found a slightly negative but insignificant relationship between average long-term SSY and the percentage of catchment area covered by easily erodible loess deposits (Haase et al., 2007) (Fig. S3). Furthermore, mean and median long-term SSY is not significantly correlated with differences in the catchments' share of agricultural areas and forests and seminatural areas, here based on Corine Land Cover data from 1990 (Fig. S3, Table 1). Similar to the fraction of impervious surfaces, the share of artificial surfaces from Corine Land Cover 1990, also including green urban areas (Table 1), shows a significant positive correlation with SSY (Fig. S3).

Overall, mean and median long-term SSY were significantly higher for the stations along the Neckar (RKN, POP and DEZ, Fig. 1) than for stations with similarly sized catchments along the other surveyed rivers (Table 2, Figs. 2, S4). At first glance, stations located along individual river systems, i.e. stations in the Main and Neckar catchments, were characterized by long-term SSY of similar magnitude. However, the Werra and Fulda, two tributaries of the Weser, showed a factor two difference in long-term SSY, despite very similar catchment size, relief and MAP (Table 2, Figs. 2, S4). While the station with the largest catchment area (RKN) showed the lowest mean long-term SSY along the Neckar, we found increasing long-term SSY with increasing catchment area in the Main river.

4.2. Hydrograph separation and spatio-temporal variability of sediment transport

On average, the stormflow index (SFI), i.e. the percentage of total discharge during our observation period attained by stormflow, ranged between 55 and 74 % following the Pelletier and Andréassian (2020) approach and between 43 and 61 % using the Lyne and Hollick (1979) approach, respectively (Table 3). Though numbers varied with a mean of ~13 % between the two different approaches, the general pattern of rivers with higher and lower stormflow contribution remained the same. The river Lahn at Kalkofen (KLK) consistently showed the highest estimated stormflow contributions, while the river Weser at Bodenwerder (BDW) constituted the lower end of the distribution.

Combining daily stormflow with daily SSL data, we estimated the long-term SSL attained by stormflow to range from 60 to 85 % and from 50 to 76 %, based on the Pelletier and Andréassian (2020) and the Lyne and Hollick (1979) approach, respectively (Table 3). Also here, the former approach consistently yielded higher estimates, but the overall pattern as well as the relative differences between the stations remained

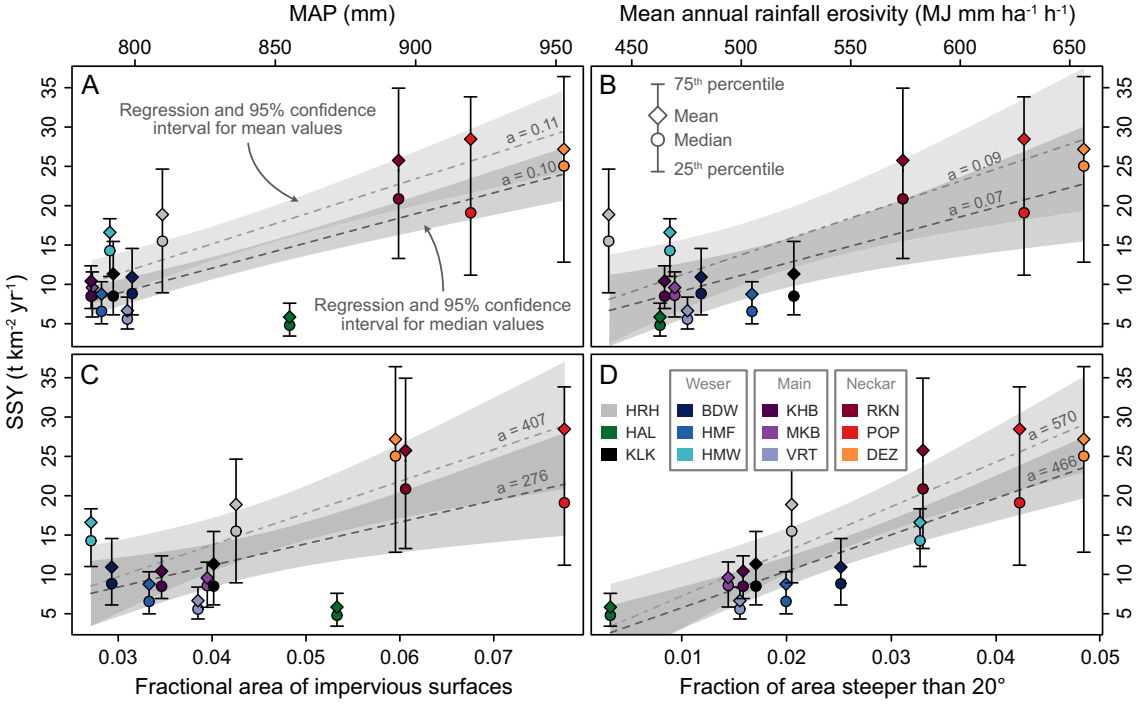

Fig. 2. Mean (circles) and median (diamonds) annual specific sediment yield (SSY), colour-coded by river systems (Fig. 1), versus (A) mean annual precipitation (MAP), (B) mean rainfall erosivity (Ballabio et al., 2017), (C) fractional area of impervious surfaces (EEA (European Environment Agency), 2020c), and (D) the fraction of upstream area with slopes steeper than 20°. Whiskers show 25th and 75th percentile of annual specific sediment yield at each station, dashed and dash-dotted line show significant (level = 0.05) robust regression of median and mean values, respectively; grey shading indicates 95 % confidence interval, grey text along dashed lines gives regression slope *a*.

Table 3
Stormflow characteristics for twelve stations along German upland rivers. Stormflow index (SFI), calculated following Pelletier and Andréassian (2020) (P&A) and Lyne and Hollick (1979) (L&H), is defined as the average percentage of total discharge attained by stormflow. Stormflow suspended sediment load (SSL) gives the percentage of long-term (observation period) SSL transported by event discharges and was calculated using daily stormflow estimates in combination with daily SSL.

Station name	Station name abbreviation	ID	River	SFI (%)		Stormflow SSL (%)	
				P&A	L&H	P&A	L&H
Deizisau	DEZ	220	Neckar	70.5	53.9	84.2	74.8
Poppenweiler	POP	221	Neckar	70.4	54.1	83.7	73.4
Rockenau	RKN	222	Neckar	65.6	52.1	82.4	73.9
Viereth	VRT	231	Main	57.2	46.3	63.5	54.2
Marktbreit	MKB	232	Main	58.2	46.7	66.8	57.3
Kleinheubach	KHB	233	Main	60.2	48.4	70.4	60.3
Kalkofen	KLK	241	Lahn	73.8	60.9	85.0	76.1
Hamm	HAL	277	Lippe	61.5	46.9	68.8	55.1
Hann.-Münden	HMW	401	Werra	61.4	47.1	66.4	53.6
Hann.-Münden	HMF	402	Fulda	61.1	49.9	69.0	59.4
Bodenwerder	BDW	403	Weser	54.6	43.4	60.4	50.2
Herrenhausen	HRH	421	Leine	57.1	47.0	69.0	59.5

nearly identical. Again, the stations KLK at the Lahn river and BDW at the Weser river bracket the distribution at the upper and lower end, respectively. Strikingly, the neighbouring catchments of the Neckar and Main rivers indicated very different behaviour, with the stormflow contribution to total suspended sediment transport at the Neckar stations roughly 20 % larger, as for the Main stations. Naturally, the percentage of stormflow contribution to annual discharge was highly variable, falling below 50 % (60 % for Lyne and Hollick) in some catchments for very dry years, while contributing up to 90 % in other catchments during very wet years (Fig. 3).

Apart from sharp long-term contrasts between monitoring stations and river catchments, our data also revealed large inter-annual variability of annual SSY at individual stations (Figs. 3, S2). For some stations, namely along the Main and Werra rivers, the coefficient of variation (CoV) in SSY clustered around 50 %. The remaining stations showed higher inter-annual variability in SSY with CoV values of around 60 to 70 %. The Neckar river at POP attained the highest CoV value of >100 %, characterized by much larger inter-annual variability than the remaining stations. In contrast to annual SSY, the variability of MAP within the catchments investigated here was much smaller, with CoV consistently falling between 14 and 18 % (Fig. S2). Sharp contrasts of high and low SSY were sometimes observed in consecutive years, e.g. in 2002/03 for the entire study region, as well as 1981/82 in northern and 1988/89 in southern Germany (Fig. 3). In some cases, years with high annual SSY coincided with large floods in Central Europe, such as the 1993 floods of the Rhine system that affected the stations along Lahn and Neckar rivers, and the March 1988 floods sticking out at the Neckar and, to a lesser degree, at the Main stations. To assess the degree to which these flood events exert a primary control on annual suspended sediment transport, we took a closer look on the intra-annual variability of SSL.

At all stations, suspended sediment transport followed a clear seasonal pattern: while the bulk of annual SSL was exported between November and April, only smaller fractions were transported from May to October (Figs. 4, S5 to S8). This general pattern also characterizes the different discharge components, with stormflow clearly dominating the average SSL during the winter and spring seasons, while summer and early autumn saw a more balanced contribution of stormflow and baseflow. This pattern closely followed the annual cycle of evapotranspiration that reduces the effective precipitation during summer months, despite high monthly precipitation amounts (Figs. 4, S5 to S8). At some stations, namely BDW, HMW, and VRT, average stormflow contribution to SSL dropped below the average baseflow contribution for several months during the summer. In contrast, for the stations along the Neckar river, average stormflow remained dominant during May, June, and July. In individual years, the Neckar stations recorded between 50 and 70 % of annual SSL during these months attained by stormflow (Figs. 4, S8). Significantly elevated stormflow sediment transport during summer months was also observed for the remaining rivers in a few years, though rarely exceeding 25 % of the annual SSL (Figs. 4, S5 to S7). Notably, along the Neckar and Lahn rivers, between 0.23 and 0.32 months per year exceeded a 50 % share of annual SSL by stormflow, i.e. having a return period of roughly three to four years. In contrast, months delivering more than half of the annual SSL had return periods exceeding ~15 years for the remaining stations.

Individual months that transport high fractions of the annual SSL temporally coincided with major floods in German rivers. In December 1993, when a severe flood affected the Rhine catchment, we found that at RKN and MKB 70 to 80 % and 50 to 60 % of the annual SSL were transported, respectively. Furthermore, though not associated with extreme stages all over Germany, but affecting large parts of the country, the floods of January 2011 coincided with elevated monthly shares of annual SSL at all stations, ranging between 40 and 80 % (Figs. 4, S5 to S8).

4.3. *Extreme suspended sediment transport events and their hysteresis patterns*

Ranking daily SSL data from largest to smallest, we constructed cumulative distributions of sediment transport for the twelve stations (Fig. 5) and calculated the time needed for different percentages of the long-term SSL to be exported from the catchments. We observed strong differences between stations: While for the Neckar (DEZ, POP, RKN) and Lahn stations (KLK) 50 % of the long-term SSL were transported in 0.6 % to 1.8 % of the observation time, the remaining stations required 4.8 % to 8.7 % of the time to export half of the total suspended sediment flux. Exceptional in this regard was the station Poppenweiler (POP), where >8 % of the long-term SSL were delivered in only two consecutive days during a flood in May 1978.

To shed light on the importance of SSTE, rather than looking into single sediment transport days that might be attributed to single flood events, we ranked the n-largest events in decreasing order and found distinct differences in their cumulative contribution to long-term SSL. While for the Neckar (DEZ, POP, RKN) and Lahn (KLK) stations suspended sediment exported by the n-largest SSTE accounted for 49 to 62 % of the long-term SSL, these estimates were between 30 and 40 % for the remaining stations (Fig. 6A). When considering the single largest SSTE, the Neckar stations again ranked highest, with between 3.1 and 9.9 % of the long-term SSL exported, followed by the station VRT on the Main river with 2.3 %. For the ten largest SSTE, the share of the long-term SSL was between ~28 % in the Neckar (DEZ, POP) and ~8 % in the Lippe and Werra rivers (Table S2).

For each identified SSTE, we cumulated the share of catchment area that received >20 mm daily precipitation over five antecedent days

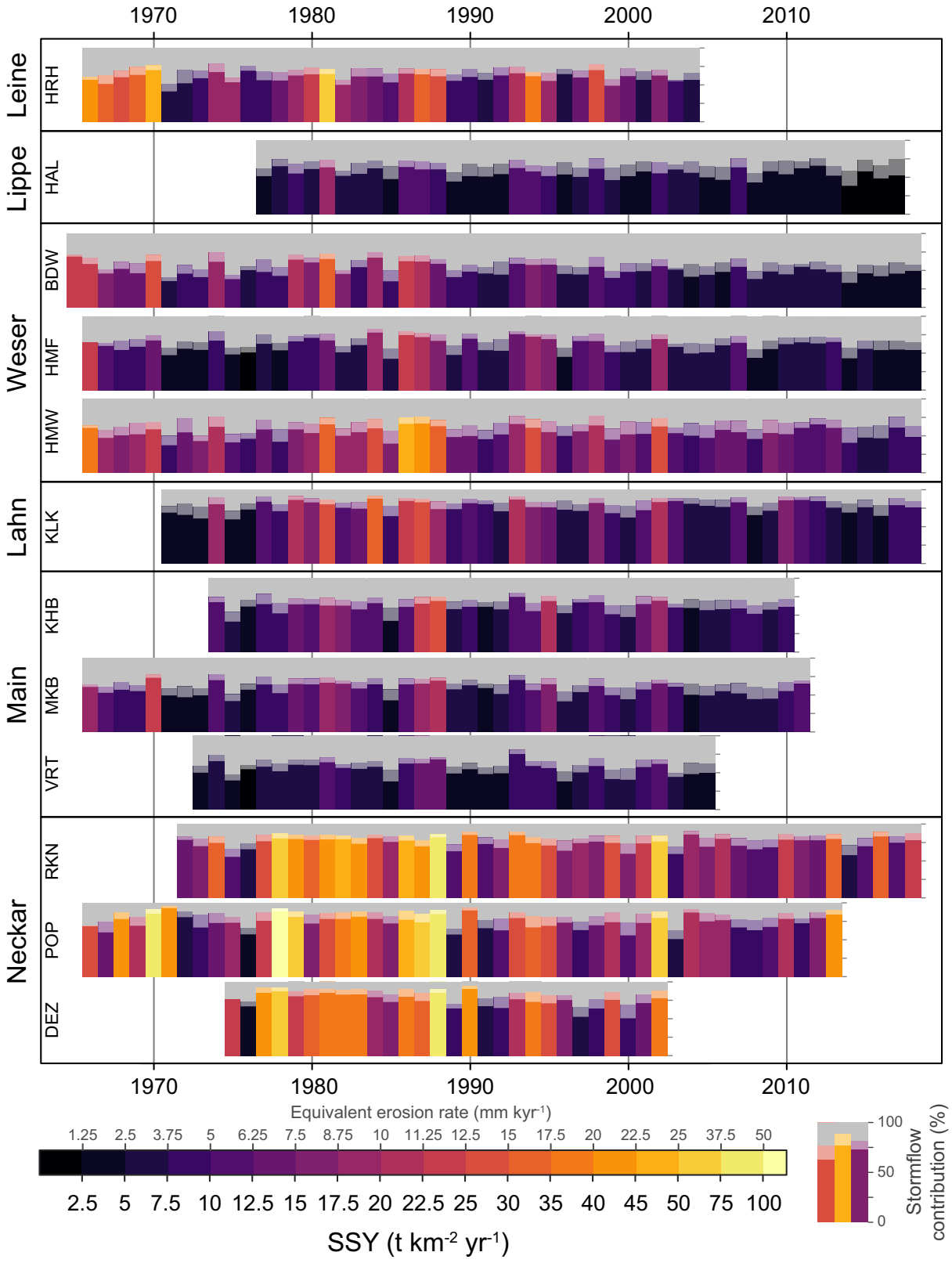

Fig. 3. Colour coded annual specific suspended sediment yield (SSY) for twelve monitoring stations in Germany between 1965 and 2018. Bar length represents the annual stormflow contribution to suspended sediment load (SSL) estimated using two different approaches, Lyne and Hollick (1979) shown in full colours and Pelletier and Andréassian (2020) indicated in pale shading, respectively (see text for details). For comparison, we converted annual SSY to equivalent erosion rates in mm kyr^{-1}, using a bulk density of 2.0 t m^{-3}. See Fig. 1 for location of stations and rivers shown here.

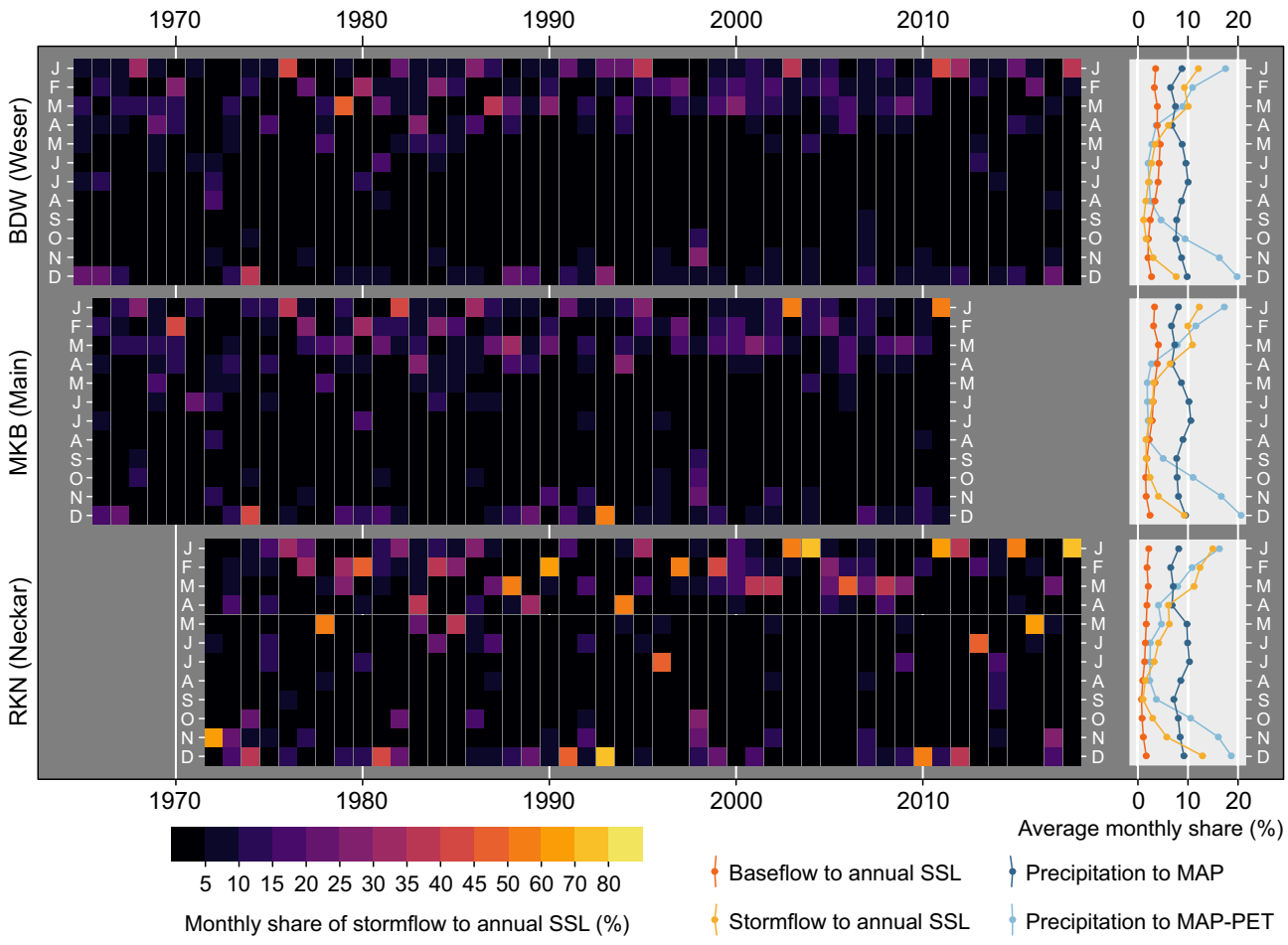

Fig. 4. Monthly suspended sediment load (SSL) by stormflow at the three stations Bodenwerder (BDW), Marktbreit (MKB) and Rockenau (RKN), colour coded by the monthly percentage of the total annual SSL. Graphs on the right show average monthly share of baseflow and stormflow to annual SSL in red and yellow, respectively and average share of monthly precipitation and monthly effective precipitation to mean annual precipitation (MAP) in blue and light-blue, respectively. Analogous figures for all stations are shown in Figs. S5 to S8. Note that the three stations shown here have roughly comparable catchment sizes (Table 1).

(Fig. 6B) as a measure of affected area of extreme precipitation. With between 42 and 65 % of the catchment area receiving >20 mm d^{-1} in the five antecedent days, the Neckar and Lippe catchments showed the highest mean coverage of intensive precipitation for the n-largest SSTE. For the remaining catchments, the precipitation intensity was significantly lower, with averages of between 15 and 32 % of the catchment area receiving >20 mm d^{-1} in the five antecedent days (Fig. S9).

Regarding the hysteresis effects during SSTE, clockwise hysteresis dominated the overall picture, but a closer look revealed systematic differences between the investigated catchments (Fig. 6C). While some catchments were clearly dominated by positive (clockwise) hysteresis, namely HRH, BDW, HAL, and KLK (all more than two thirds positive), the remaining catchments showed a more balanced distribution, but mostly with a tendency towards positive hysteresis effects. Only for the station POP, and to a lesser extent RKN, anti-clockwise hysteresis effects prevailed (Fig. 6C). In terms of SSL exported during the n-largest SSTE, clockwise hysteresis clearly dominated: for eleven stations >50 % of SSL was attained during events with positive hysteresis loops, at four stations (HAL, HRH, BDW, KLK) even accounting for more than three quarters of the total SSL. Only for the station POP, 69 % of the SSL was transported during SSTE with a negative hysteresis loop.

At all stations, the majority of SSTE occurred during the hydrological winter season, for Germany defined as from 1st November to 30th April. At the stations KLK, HMF, HAL, HRH, VRT and KHB the hydrological summer season only saw between 10 and 12 % of the n-largest floods in terms of sediment transport, while along the Neckar river, and also the station HMW, this figure was between 18 and 35 % (Fig. S9). Despite the dominance of positive and negative hysteresis loops in different catchments, we did not detect any seasonal pattern in hysteresis effects.

5. Discussion

Here we first discuss the spatial differences of suspended sediment dynamics between the surveyed catchments and their within-catchment variability on inter-annual times scales, before addressing the relative contribution of stormflow and baseflow as well as the importance of extreme events for long-term sediment transport in the second part.

5.1. *Spatio-temporal variability of long-term and inter-annual suspended sediment yield*

In relation to an inventory of 1794 entries covering large parts of the European continent, average SSY for twelve stations along German upland rivers (6.8 and 28.7 t km^{-2} yr^{-1}, Fig. 2, Table 2) ranks in the lower quartile (Vanmaercke et al., 2011). This is also the case in comparison to a global data set that finds average SSY between 50 and 100 t km^{-2} yr^{-1} for catchments on the 10^3 to 10^4 km^2 scale (García-Ruiz et al., 2015). However, global or continental data sets comprise a broad range of topo-climatic settings. But also in relation to sites with roughly comparable relief and precipitation patterns from the UK and France, where SSY estimates are between 24 and 45 t km^{-2} yr^{-1} (Harlow et al., 2006) and between 9 and 186 t km^{-2} yr^{-1} (Maneux et al., 2001; Oeurng et al.,

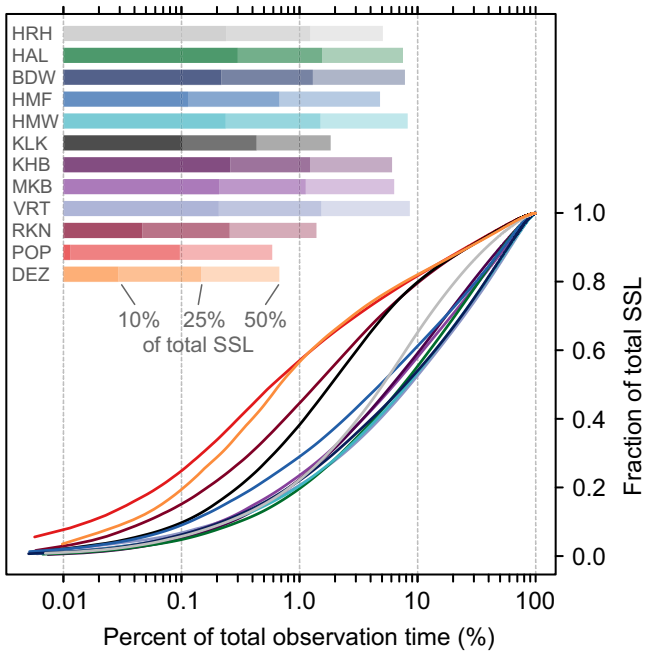

Fig. 5. Cumulated total suspended sediment load for twelve monitoring stations between 1966 and 2018, colour-coded by river systems (Fig. 1), see Table 2 for abbreviated station names. Note that percentage of observation time on the x-axis is shown on a logarithmic scale.

2010), respectively, average rates found for the German upland regions are in the lower ranges. Still, it has to be noted that most of the data cited above is derived from significantly shorter time series, spawning large uncertainties on SSY estimates. Moreover, the majority of catchments surveyed by these studies is significantly smaller than in our data set, and higher rates might be associated with the reduced storage capabilities and the resulting high degree of connectivity between hillslopes and river channels of these river systems (García-Ruiz et al., 2015; Walling, 1983).

But also in the context of averaged denudation rates on 10^3–10^4 year time scales that span the range from ~37 to 112 mm kyr^{-1}, derived from sediment budget approaches and cosmogenic radionuclide abundances in river sands (Hoffmann et al., 2007, 2013; Houben, 2012; Schaller et al., 2001; Seidel and Mäckel, 2007), the decadal rates found in our study are significantly lower. Converting average SSY to equivalent denudation rates using a bulk density of 2.0 t m^{-3}, our data translate to 3.4 to 14.4 mm kyr^{-1} of average surface lowering. However, we stress here that our rates are solely derived from suspended sediment monitoring and do neither include bedload transport nor solute transport of erosional products. While bedload contribution to modern sediment transport in upland rivers of Germany is negligible due to the disruption of longitudinal transport by barrages, dissolved load might exceed suspended load in the Neckar catchment (Schaller et al., 2001). Furthermore, Hoffmann et al. (2013) point out that discrepancies between modern and long-term denudation rates on the 10^3–10^4 year time scales might be owed to the storage of large fractions of eroded soils (~50 % at the Holocene time scale) on hillslopes that hence do not contribute to the sediment supply to river systems.

It is important to note that the data used here does not differentiate between mineral and organic suspended material, thus representing total suspended matter including both components in the estimation of SSL and SSY. However, we are confident that organic matter plays a subordinate role in our estimates for two reasons: First, in all river systems surveyed, gross sediment transport is focused on the winter season, when organic matter concentration is usually low. Second, Hoffmann et al. (2020) showed the share of organic matter to be inversely correlated with discharge in German upland rivers. In this sense, suspended organic matter might constitute a significant portion of summer-season SSL, but likely only accounts for a small fraction of the annual and long-term sediment transport as measured at the twelve stations investigated here.

Though we cannot directly link across-catchment differences in average SSY to individual controlling factors, elevated rainfall erosivity and a high fractional area of slopes steeper than 20° (Fig. 2B, D) likely exert a first-order control. This notion is supported by significant correlations between SSY and additional topographic metrics (Fig. S3), that corroborate earlier findings (Schaller et al., 2001). Higher mean annual precipitation favours high rainfall erosivity and is thus also related to SSY in Fig. 2. The significant differences in fractional area of steep slopes between the neighbouring Werra and Fulda rivers and the Neckar and Main rivers seems to control their contrasting long-term SSY. In the case of the adjacent Neckar and Main rivers, reduced precipitation amount and intensity in the Main catchment further enhance the differences in sediment transport (Fig. 2). In contrast to earlier studies that link catchment sediment transport to land cover distribution (Montgomery, 2007; Vanmaercke et al., 2015), neither the share of agricultural areas nor the percentage of forests and seminatural areas seem to exert a primary control in our study (Fig. S3). However, it has been shown that while the impact of land use on sediment transport might be dominant on the small scale, it becomes marginal in catchments of $>10^3$ km^2 (Vanmaercke et al., 2015). Furthermore, the share of agricultural land in the catchments surveyed here is narrowly confined between 49 and 59 % (exception Lippe catchment, Table 1), which might explain why topoclimatic parameters are more important here. The intriguing correlation between average SSY and the fraction of impervious surfaces (Fig. 2) is supported by the findings of earlier studies (Carter et al., 2003; Taylor and Owens, 2009). Urban street dust (and additional particles) that accumulates over dry periods in the summer might constitute a significant portion of total SSC and SSL, especially during convective events in the summer season (Vercruysse and Grabowski, 2019). However, we stress here that despite their significance, the direction of correlations shown in Fig. 2 A, B, and C might well point into the opposite direction, if the Neckar samples are not taken into account. In turn, the positive trend between SSY and the fractional area of slopes steeper than 20° is more robust and holds even without the Neckar stations, suggesting a strong topographic influence on sediment transport.

In this context it is important to consider the influence of the observation time-scale. Compressed variance is a known effect in short term data series, associated with large errors in estimates of mean sediment transport rates and underestimates the role of extreme events (García-Ruiz et al., 2015; Gonzalez-Hidalgo et al., 2010). For a meta-analysis of global soil erosion data, García-Ruiz et al. (2015) find decreasing standard errors of mean erosion rates with increasing observation period and recommend a minimum of 20 years of observation for robust estimates. We are confident that our suspended sediment yield estimates are not influenced by the effect of compressed variance, as our data covers between 28 and 54 years of daily observations.

SSY from the twelve catchments surveyed here is strongly driven by inter-annual rainfall variability. Overall, catchment averaged precipitation and SSY are closely correlated for large parts of our observation timescale in most of the rivers, underlining the climatic influence on SSY (Fig. S10). Especially for the Neckar and Leine catchments, we find the highest inter-annual variability, where very wet years coincide with increased sediment dynamics (Figs. 3, S2). However, SSY is characterized by much higher CoV compared to the CoV of catchment averaged MAP, indicating a strong non-linear increase of SSY with MAP (Fig. S2) that further complicates future predictions of sediment transport in the wake of increasing precipitation in a changing climate (Feldmann et al. 2013). Despite observed positive discharge trends for the Rhine and Weser river systems (Bormann, 2010) and an increase in rainfall erosivity (Fiener et al., 2013), Hoffmann et al. (2022) report a significant

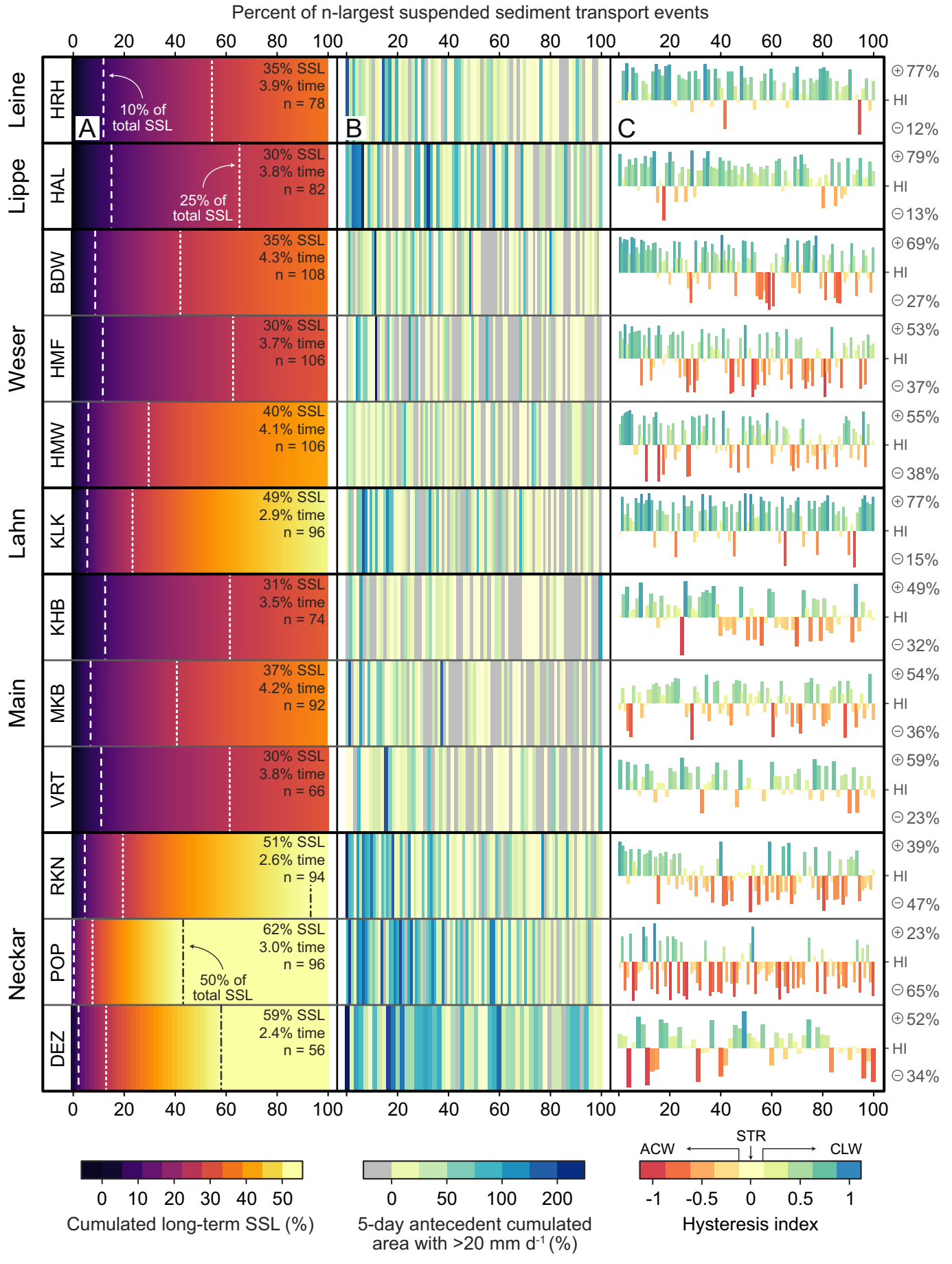

(caption on next page)

Fig. 6. Sediment transport (A), rainfall intensity (B) and hysteresis effects (C) of the n-largest ($n = 2 \times$ observation period in years) suspended sediment transport events (SSTE) in descending order. (A) Barplot of the n-largest SSTE colour-coded by their cumulated percentage of long-term suspended sediment load (SSL). Dashed and dotted white lines mark the position of the 10th and 25th percentile, respectively, dash-dotted grey line indicates 50th percentile of long-term SSL. Numbers on the right indicate total percentage of SSL attained by n-largest events, total percentage of observation time covered by the n-largest events and respective number of n-largest events for each station. (B) Colour-coded representation of the cumulated percentage of study area that received rainfall exceeding 20 mm d^{-1} (REGNIE data) in the five days prior to the SSL peak. (C) Hysteresis index (HI) for n-largest SSTE. More negative values indicate more pronounced anti-clockwise (ACW) hysteresis, more positive values relate to clockwise (CLW) hysteresis, and values close to zero approach straight or complex (STR) hysteresis patterns. Y-axis in (A) and (B) are dimensionless, in (C) scaled from −1 to 1, x-axis for all panels shows percentage of n-largest SSTE. Numbers on the right y-axis give percentages of positive and negative hysteresis loops, defined here by a HI above 0.1 and below −0.1, respectively.

decline in sediment loads for a larger station network in German river systems over the past decades that is also apparent in our data (Figs. 3, S2). However, further investigating these long-term trends and their controlling factors is beyond the scope of the present study and we refer to the extensive discussion in Hoffmann et al. (2022).

A crucial point to consider when investigating sediment transport in Central Europe is the human alteration of river channels, floodplains and entire drainage catchments that affects sediment dynamics in managed river systems (Tockner et al., 2009; Wohl, 2015). In the past 200 years, practically all river channels in Central Europe were subject to river engineering, erosion control and flood protection of varying degrees. For Germany it is estimated that on average between 1.72 and 2.16 barriers interrupt longitudinal sediment transport per river kilometre (Belletti et al., 2020), including barrages along major waterways and more frequent small-scale constructions (e.g. flood retention basins) in low-order headwater catchments. Together, these barriers along Central European waterways retain a significant fraction of the SSL. For instance along the Upper Rhine, ten barrages between Weil am Rhein and Iffezheim retain approximately 0.3 Mt. of sediment each year (Frings et al., 2019; Hoffmann et al., 2017). While most of the large in-channel barrages were constructed before the 1970ies (Hoffmann et al., 2022), their specific management might still influence SSC along German waterways. In addition, the combined effect of larger water reservoirs in the headwaters (Speckhann et al., 2021) and a large number of small-scale features may strongly control the link between SSY and MAP.

5.2. Stormflow contribution, extreme events and hysteresis effects

The share of total sediment transport achieved during stormflow runoff varies by 25 % between the surveyed rivers, but does not necessarily mirror the variability of long-term SSY (Tables 2, 3). Since delayed baseflow is sourced from different storages, like subsurface flow and aquifers, catchment lithology and floodplain configuration likely explain large parts of the variability in stormflow contribution to sediment transport (Hall, 1968; Smakhtin, 2001). In addition to these hydrogeological boundary conditions, the stations along the Neckar and Lahn rivers that show the highest share of total SSL transported during stormflow discharges are also characterized by elevated precipitation intensities (Figs. 6, S9, S11), potentially contributing to the dominant role of stormflow there. While baseflow only shows a dampened seasonality, distinct seasonality of stormflow sediment transport found for all catchments (Figs. 4, S5-S8) indicates a dynamic relationship between discharge and sediment load that is governed by seasonal variations in driving factors, including precipitation amount and intensity, effective precipitation, as well as vegetation cover (Sun et al., 2016; Vercruysse et al., 2020). Opposed to an earlier study reporting sediment exhaustion effects over the hydrological year in the Exe river, UK, with SSL peaking in winter and already declining in early spring (Harlow et al., 2006), the seasonal pattern found here shows a clear tendency to have the highest sediment loads in the first quarter of the calendar year. We interpret this as the effect of elevated effective precipitation that increase soil moisture over the winter season, reduced natural vegetation and crop coverage, as well as snow melt in upland regions during this time of the year, all pointing to transport-limited conditions. While most stations also show a very similar behaviour during the late spring and early summer seasons, in the Neckar catchment consistently higher monthly contribution of SSL during April, May and June coincides with a significantly higher average number of days with >20 mm of precipitation (Fig. S11). In accordance with this observation, the Neckar catchment shows the highest rainfall erosivity during the summer months (Ballabio et al., 2017). This suggests that high intensity and/or long-duration precipitation, the latter taken as a proxy for soil moisture, exert a first-order control on sediment dynamics here (Seeger et al., 2004; Vercruysse et al., 2020). For the decades to come, MAP, precipitation extremes as well as average rainfall erosivity are projected to increase over Germany (Feldmann et al. 2013, Panagos et al., 2017), likely impacting magnitude and seasonality of future suspended sediment transport.

Strikingly, several months that transport a significant share of the annual sediment load at the stations along the Neckar river (Fig. 4) coincide with documented landslides along the escarpment of the Swabian cuesta landscape. The largest landslide reported during the observation period happened in 1983, an estimated volume of 6 * 10^6 m^3 was released from the Hirschkopf on 12 April (Bibus, 1986) after a wet winter season and days of heavy rainfall that delivered one third of the annual rainfall. Furthermore, 26 landslides were documented along the Swabian Alb and their foreland (Bell, 2007), likely triggered by heavy rainfalls on 22 March 1988. Finally, multiple landslides of up to 0.5 Mm^3 (https://www.lgrb-bw.de) were triggered following heavy rainfalls in the first days of June 2013 (Eberle et al., 2017) (Fig. 4).

Most prominent, however, were the flash floods and debris flows affecting the village of Braunsbach at the Kocher river, a tributary to the Neckar. In late May 2016, heavy rainstorms delivered >100 mm in about 2 h to the small (~6 km^2) catchment of the Orlacher Bach, generating a flash flood and a series of destructive debris flows that exported a record-breaking 14 kt km^{-2} (Bronstert et al., 2018; Ozturk et al., 2018). Though we note here that the Braunsbach catchment was not the only locality receiving extreme precipitation amounts in late May and early June 2016, we stress that extreme localized sediment input to the Kocher catchment on 29 May is connected to the second highest daily sediment load on record that passes the station RKN on 30 May 2016, located ~100 km downstream (Table S2). Whether localized extreme events such as the Braunsbach case and landslide clusters along the Swabian Alb escarpment exert a dominant control on sediment transport of intermediate and large river catchments, or are merely the most extreme expression of regional rainfall patterns inducing surface erosion in a larger region, remains unresolved. In either case, we emphasize here that despite the tendency of sediment pulses to be attenuated downstream, either due to dilution effects from tributary inputs or sediment storage within channels and floodplains (Asselman, 1999), localized extreme events can dominate the annual sediment flux for hundreds of kilometres, as witnessed by the Braunsbach example in the Neckar catchment. Still, the question remains whether or not such extreme SSTE are significant for total sediment transport on decadal to centennial time scales.

In this respect, the overall contribution of the single largest flood in the Neckar catchment, responsible for nearly 10 % of the long-term SSL in May 1978, seems exceptional. This is not only because it exceeds the fraction of long-term SSL achieved by the largest flood at the remaining stations by far, ranging between 1.0 and 5.3 % (Table S2). At the gauging station Plochingen, located between stations POP and DEZ, the flood of May 1978 is also the highest on record (starting 1921), with a

peak discharge of 1150 m^3 s^{-1}, only surpassed by reconstructed flood discharges during the 19th century (Seidel et al., 2012). Furthermore, maximum measured SSC during this event attained a value of 3450 mg L^{-1}, exceeding maximum values for the remaining stations by >25 % and exceeding the long-term mean SSC by a factor of >100. However, we emphasize that daily sampling, and even averaging three individual samples during flood situations, cannot fully represent the short-term variability of suspended sediment concentration during single flood events that cause rapid changes of Q and SSC (Naden, 2010). In comparison to earlier studies assessing the importance of the highest daily sediment load for average sediment transport, our study yields comparable results (Gonzalez-Hidalgo et al., 2010). The discrepancy between ~80 % of long-term SSL that is exported in <10 % of observation time for the Neckar and Lahn rivers, and in between 20 and 40 % of time in the other catchments studied here is remarkable (Fig. 5). We attribute this to the combined non-linear effects of topography, rainfall erosivity and precipitation intensity (Figs. 2, 6, S1, S11). The catchment lithology likely constitutes an additional factor that influences suspended sediment transport, as indicated by the predisposition of the Swabian cuesta landscape towards gravitational mass movements, providing large amounts of fine-grained sediments ready for mobilization during extreme rainfall events. However, a thorough analysis of lithological differences and how they influence discharge characteristics of the river systems surveyed here remains beyond the scope of our study.

It is a long-standing hypothesis that flood waves travel at higher speeds than sediments, introducing a progressive lag between water and sediment peaks with increasing catchment size (Heidel, 1956). This introduces the effect that clockwise hysteresis often dominate upstream sections of river networks, while progressively shifting towards anti-clockwise hysteresis in the lower reaches (Marcus, 1989; Tena et al., 2014). However, at the scale of the catchments surveyed here, we cannot observe such a pattern. In contrast, and in line with studies from medium sized catchments, clockwise hysteresis patterns dominate sediment transport events in our study region, while counter-clockwise hysteresis plays a minor role (Misset et al., 2018; Oeurng et al., 2010). Clockwise hysteresis is commonly taken as an indication for sediment entrainment from within the channel or from proximal sources, whereas anti-clockwise hysteresis rather indicate distant sediment sources (Klein, 1984). In this sense, the dominance of clockwise hysteresis loops at most stations investigated here might indicate a major role of re-entrainment of previously stored in-channel sediments during flood events in the sediment dynamics in German waterways. Clockwise hysteresis patterns are also dominant in the Rhine river, where fine sediments get temporarily stored during summer low flows, acting as sediment sources in the winter season (Asselman, 1999). In-channel storage and remobilization during floods in the considered river systems is strongly conditioned by barrages along the surveyed rivers, increasing the likelihood of clockwise hysteresis through sediment remobilization during the rising limb of floods and rapid exhaustion of in-channel sediments, also making streambed erosion possible during such events. The conspicuous dominance of clockwise hysteresis in the largest floods at most stations might point to such an effect on sediment dynamics. Data from earlier studies that found a dominance of anti-clockwise hysteresis for the largest events, interpreted as floods of sufficient magnitude to activate and transport distant sources (Haddadchi and Hicks, 2021; Oeurng et al., 2010), further support this notion. On the other hand, the dominance of anti-clockwise hysteresis in the Neckar catchment at POP and, to a lesser extent, RKN is noteworthy. It might well be that higher mean annual precipitation, mean annual rainfall erosivity, general terrain steepness, and fraction of impervious surfaces (Fig. 2), combined with more frequently occurring precipitation events exceeding 20 mm d^{-1} (Fig. S11) in the Neckar catchment facilitates the erosion and transport of sediments from more distant sources. A further important difference to recognize is the propensity for landsliding along the escarpment of the Swabian Alb that deliver fine grained colluvial deposits to the footslopes, where fluvial processes entrain these sediments (Bell, 2007).

The climatic changes of past decades have already altered both precipitation patterns and the frequency and magnitude of extreme events (Kunz et al., 2017; Zeder and Fischer, 2020). It remains to be seen whether extreme sediment transport events such as Braunsbach and the devastating floods in the Ahrtal during the summer 2021 (Bronstert et al., 2018; Kreienkamp et al., 2021) will also increase in magnitude and/or frequency and shift the current sediment transport regime of German upland rivers to an even greater dominance of extreme events, which is not only relevant from a natural hazards perspective, but might also critically impact river ecology and fluvial morphodynamics.

6. Conclusions

Investigating daily suspended sediment transport at twelve monitoring stations in German upland rivers on decadal time scales revealed sharp contrasts in neighbouring river systems despite broadly comparable topo-climatic settings. For the entire monitoring period that varied between 28 and 54 years for different stations, average specific suspended sediment yield spanned the range from 5.9 for the Lippe to 28.7 t km^{-2} yr^{-1} for the Neckar river. Our data indicate that topo-climatic parameters such as rainfall amount and intensity, as well as a high fractional area of steep slopes exert a first-order control on these differences, but also additional factors, including underlying catchment geology and river management practices, come into play. The average share of total sediment load transported by stormflow discharges, that we quantified using two different streamflow separation approaches, exceeded ~73 % for the Neckar and Lahn catchments, while ranging ~15 % lower for the remaining catchments. Though this general pattern seems to be related to lithological differences that determine subsurface aquifer conditions, the clear seasonal pattern that characterized stormflow sediment transport at all stations, with the largest amount transported during the winter season, is controlled by elevated effective precipitation and reduced vegetative cover during the winter season. However, intensive precipitation events modulate this general pattern. Especially in the Neckar catchment, sediment transport events that export >50 % of the annual load occurred regularly. Overall, sediment transport events are dominated by positive (clockwise) hysteresis effects that hint to within-channel reworking as an important sediment source during floods, likely related to existence of barrages to control water levels and secure navigation along the waterways. Only for the stations along the Neckar river, a larger share of negative hysteresis effects point to the dominance of distant sediment sources, despite the strong control of flow conditions due to numerous barrages along the waterway. It is also in the Neckar catchment that we find the highest contribution of extreme sediment transport events to overall sediment load. Here 27.6 % of the long-term suspended sediment load is exported during the ten largest events, representing <0.5 % of the observation time. After all, the Neckar catchment significantly differs from the remaining stations in every respect investigated here, which we interpret as the combined effect of elevated rainfall intensity, higher fraction of steeper slopes and the landslide susceptibility of the Swabian Alb escarpment. Taken together, these factors likely control the high long-term specific sediment yield, the large inter-annual variability, the high share of sediment transported during stormflow phases as well as the importance of extreme events during the summer season. Not least the flood events of July 2021 in Western Germany have dramatically shown the vulnerability of upland regions towards extreme sediment transport events. Though not covering this particular event, our data showed the far-reaching and long-lasting impact of earlier extreme events for long-term sediment transport. Continued investigation of suspended sediment dynamics will be required to better understand and ultimately anticipate the adverse effects of sediment transport events in a changing climate.

Declaration of competing interest

The authors declare that they have no known competing financial interests or personal relationships that could have appeared to influence the work reported in this paper.

Data availability

Aggregated annual data can be made available on request to thomas.hoffmann@bafg.de

Acknowledgements

The authors would like to thank the Federal Waterways and Shipping Administration (WSV; www.wsv.de) for providing the data on suspended sediment loads. Aggregated annual data can be made available on request to thomas.hoffmann@bafg.de. Furthermore, the provision of gridded and station climate data by the Deutscher Wetterdienst (DWD Climate Data Center) and the gridded data sets under the Corpernicus framework of the EU at no cost is very much appreciated. Finally, we thank Francesco Comiti and one anonymous reviewer for their helpful comments as well as Rainer Bell, Annette Bösmeier and Klaus Vormoor for valuable suggestions during earlier stages of our work and Till Francke for sharing R-code for automated event detection.

Appendix A. Supplementary data

Supplementary data to this article can be found online at https://doi.org/10.1016/j.geomorph.2022.108462.

References

Asselman, N.E.M., 1999. Suspended sediment dynamics in a large drainage basin: the River Rhine. Hydrol. Process. 13, 1437–1450. https://doi.org/10.1002/(SICI)1099-1085(199907)13:10<1437::AID-HYP821>3.0.CO;2-J.

Asselman, N.E.M., 2000. Fitting and interpretation of sediment rating curves. J. Hydrol. 234, 228–248. https://doi.org/10.1016/S0022-1694(00)00253-5.

Ballabio, C., Borrelli, P., Spinoni, J., Meusburger, K., Michaelides, S., Beguería, S., Klik, A., Petan, S., Janeček, M., Olsen, P., Aalto, J., Lakatos, M., Rymszewicz, A., Dumitrescu, A., Tadić, M.P., Diodato, N., Kostalova, J., Rousseva, S., Banasik, K., Alewell, C., Panagos, P., 2017. Mapping monthly rainfall erosivity in Europe. Sci. Total Environ. 579, 1298–1315. https://doi.org/10.1016/j.scitotenv.2016.11.123.

Bell, R., 2007. Lokale und regionale Gefahren- und Risikoanalyse gravitativer Massenbewegungen an der Schwäbischen Alb (Dissertation). Bonn.

Belletti, B., Garcia de Leaniz, C., Jones, J., Bizzi, S., Börger, L., Segura, G., Castelletti, A., van de Bund, W., Aarestrup, K., Barry, J., Belka, K., Berkhuysen, A., Birnie-Gauvin, K., Bussettini, M., Carolli, M., Consuegra, S., Dopico, E., Feierfeil, T., Fernández, S., Fernandez Garrido, P., Garcia-Vazquez, E., Garrido, S., Giannico, G., Gough, P., Jepsen, N., Jones, P.E., Kemp, P., Kerr, J., King, J., Łapińska, M., Lázaro, G., Lucas, M.C., Marcello, L., Martin, P., McGinnity, P., O'Hanley, J., Olivo del Amo, R., Parasiewicz, P., Pusch, M., Rincon, G., Rodriguez, C., Royte, J., Schneider, C.T., Tummers, J.S., Vallesi, S., Vowles, A., Verspoor, E., Wanningen, H., Wantzen, K.M., Wildman, L., Zalewski, M., 2020. More than one million barriers fragment Europe's rivers. Nature 588, 436–441. https://doi.org/10.1038/s41586-020-3005-2.

Bibus, E., 1986. Die Rutschung am Hirschkopf bei Mössingen (Schwäbische Alb). Geowissenschaftliche Rahmenbedingungen - Geoökologische Folgen. Geoökodynamik 7, 333–360.

Bormann, H., 2010. Runoff regime changes in German rivers due to climate change. ERD 64, 257–279. https://doi.org/10.3112/erdkunde.2010.03.04.

Bronstert, A., Agarwal, A., Boessenkool, B., Crisologo, I., Fischer, M., Heistermann, M., Köhn-Reich, L., López-Tarazón, J.A., Moran, T., Ozturk, U., Reinhardt-Imjela, C., Wendi, D., 2018. Forensic hydro-meteorological analysis of an extreme flash flood: the 2016–05-29 event in Braunsbach, SW Germany. Sci. Total Environ. 630, 977–991. https://doi.org/10.1016/j.scitotenv.2018.02.241.

Carter, J., Owens, P.N., Walling, D.E., Leeks, G.J.L., 2003. Fingerprinting suspended sediment sources in a large urban river system. Sci. Total Environ. 314–316, 513–534. https://doi.org/10.1016/S0048-9697(03)00071-8.

Cleveland, W.S., 1979. Robust locally weighted regression and smoothing scatterplots. J. Am. Stat. Assoc. 74, 829–836. https://doi.org/10.1080/01621459.1979.10481038.

Death, R.G., Fuller, I.C., Macklin, M.G., 2015. Resetting the river template: the potential for climate-related extreme floods to transform river geomorphology and ecology. Freshw. Biol. 60, 2477–2496. https://doi.org/10.1111/fwb.12639.

Deumlich, D., Gericke, A., 2020. Frequency trend analysis of heavy rainfall days for Germany. Water 12, 1950. https://doi.org/10.3390/w12071950.

DWD (Deutscher Wetterdienst) Climate Data Center (CDC), 2020. REGNIE grids of daily precipitation. available at. https://opendata.dwd.de/climate_environment/CDC/grids_germany/daily/regnie/.

DWD (Deutscher Wetterdienst) Climate Data Center (CDC), 2020. REGNIE grids of monthly precipitation. available at. https://opendata.dwd.de/climate_environment/CDC/grids_germany/monthly/regnie/.

DWD (Deutscher Wetterdienst) Climate Data Center (CDC), 2021. Historical daily station observations for Germany, version v21.3. available at. https://opendata.dwd.de/climate_environment/CDC/observations_germany/climate/daily/kl/historical/.

Eberle, J., Eitel, B., Blümel, W.D., Wittmann, P., 2017. Deutschlands Süden - vom Erdmittelalter zur Gegenwart. Springer Berlin Heidelberg, Berlin, Heidelberg. https://doi.org/10.1007/978-3-662-54381-8.

EEA (European Environment Agency), 2020. Corine Land Cover Version 1990 © European Union. Copernicus Land Monitoring Service.

EEA (European Environment Agency), 2020. EU-DEM v1.1 © European Union. Copernicus Land Monitoring Service.

EEA (European Environment Agency), 2020. Imperviousness 2015 © European Union. Copernicus Land Monitoring Service.

Fiener, P., Neuhaus, P., Botschek, J., 2013. Long-term trends in rainfall erosivity–analysis of high resolution precipitation time series (1937–2007) from Western Germany. Agric. For. Meteorol. 171–172, 115–123. https://doi.org/10.1016/j.agrformet.2012.11.011.

Frings, R.M., Gehres, N., Promny, M., Middelkoop, H., Schüttrumpf, H., Vollmer, S., 2014. Today's sediment budget of the Rhine River channel, focusing on the Upper Rhine Graben and Rhenish Massif. Geomorphology 204, 573–587. https://doi.org/10.1016/j.geomorph.2013.08.035.

Frings, R.M., Hillebrand, G., Gehres, N., Banhold, K., Schriever, S., Hoffmann, T., 2019. From source to mouth: Basin-scale morphodynamics of the Rhine River. Earth Sci. Rev. 196, 102830 https://doi.org/10.1016/j.earscirev.2019.04.002.

García-Ruiz, J.M., Beguería, S., Nadal-Romero, E., González-Hidalgo, J.C., Lana-Renault, N., Sanjuán, Y., 2015. A meta-analysis of soil erosion rates across the world. Geomorphology 239, 160–173. https://doi.org/10.1016/j.geomorph.2015.03.008.

Gonzalez-Hidalgo, J.C., Batalla, R.J., Cerdà, A., de Luis, M., 2010. Contribution of the largest events to suspended sediment transport across the USA. Land Degrad. Dev. 21, 83–91. https://doi.org/10.1002/ldr.897.

Haase, D., Fink, J., Haase, G., Ruske, R., Pécsi, M., Richter, H., Altermann, M., Jäger, K.-D., 2007. Loess in Europe—its spatial distribution based on a European Loess Map, scale 1:2,500,000. Quat. Sci. Rev. 26, 1301–1312. https://doi.org/10.1016/j.quascirev.2007.02.003.

Haddadchi, A., Hicks, M., 2021. Interpreting event-based suspended sediment concentration and flow hysteresis patterns. J. Soils Sediments 21, 592–612. https://doi.org/10.1007/s11368-020-02777-y.

Hall, F.R., 1968. Base-flow recession - a review. Water Resour. Res. 4 (5), 973–983. https://doi.org/10.1029/WR004i005p00973.

Harlow, A., Webb, B., Walling, D., 2006. Sediment yields in the Exe Basin: a longer-term perspective. In: Sediment Dynamics And the Hydromorphology of Fluvial Systems. IAHS Press, pp. 12–20.

Heidel, S.G., 1956. The progressive lag of sediment concentration with flood waves. EOS Trans. Am. Geophys. Union 37, 56–66. https://doi.org/10.1029/TR037i001p00056.

Henningsen, D., Katzung, G., 2011. Einführung in die Geologie Deutschlands. Spektrum Akademischer Verlag, Heidelberg.

Hillebrand, G., 2013. Monitoring of suspended loads in waterways. In: Proceedings of the "Karlsruher Flussgebietstage 2013" - International Conference on Solids in River Basins. KIT, pp. 40–45.

Hoffmann, T., Erkens, G., Cohen, K.M., Houben, P., Seidel, J., Dikau, R., 2007. Holocene floodplain sediment storage and hillslope erosion within the Rhine catchment. Holocene 17, 105–118. https://doi.org/10.1177/0959683607073287.

Hoffmann, T., Schlummer, M., Notebaert, B., Verstraeten, G., Korup, O., 2013. Carbon burial in soil sediments from Holocene agricultural erosion, Central Europe. Glob. Biogeochem. Cycles 27, 828–835. https://doi.org/10.1002/gbc.20071.

Hoffmann, T., Hillebrand, G., Noack, M., 2017. Uncertainty analysis of settling, consolidation and resuspension of cohesive sediments in the Upper Rhine. Int.J.River Basin Manag. 15, 401–411. https://doi.org/10.1080/15715124.2017.1375509.

Hoffmann, Baulig, Y., Fischer, H., Blöthe, J., 2020. Scale breaks of suspended sediment rating in large rivers in Germany induced by organic matter. Earth Surf. Dyn. 8, 661–678. https://doi.org/10.5194/esurf-8-661-2020.

Hoffmann, T., Baulig, Y., Vollmer, S., Blöthe, J., Fiener, P., 2022. Back to pristine levels: a meta-analysis of suspended sediment transport in large German river channels. Earth Surf. Dynam. Discuss. 10 https://doi.org/10.5194/esurf-2022-45.

Houben, P., 2012. Sediment budget for five millennia of tillage in the Rockenberg catchment (Wetterau loess basin, Germany). Quat. Sci. Rev. 52, 12–23. https://doi.org/10.1016/j.quascirev.2012.07.011.

Klein, M., 1984. Anti clockwise hysteresis in suspended sediment concentration during individual storms: Holbeck catchment; Yorkshire, England. Catena 11, 251–257. https://doi.org/10.1016/S0341-8162(84)80024-7.

Kreienkamp, F., Philip, S.Y., Tradowsky, J.S., Kew, S.F., Lorenz, P., Arrighi, J., Belleflamme, A., Bettmann, T., Caluwaerts, S., Chan, S.C., Ciavarella, A., De Cruz, L., de Vries, H., Demuth, N., Ferrone, A., Fischer, Rich, M., Fowler, H.J., Goergen, K., Heinrich, D., Henrichs, Y., Lenderink, G., Kaspar, F., Nilson, E., Otto, F.E.L., Ragone, F., Seneviratne, S.I., Singh, R.K., Skålevåg, A., Termonia, P., Thalheimer, L., van Aalst, M., Van den Bergh, J., Van de Vyver, H., Vannitsem, S., van Oldenborgh, G.J., Van Schaeybroeck, B., Vautard, R., Vonk, D., Wanders, N., 2021. Rapid Attribution of Heavy Rainfall Events Leading to the Severe Flooding in Western Europe During July 2021. World Weather Attribution.

Kunz, M., Mohr, S., Werner, P.C., 2017. Niederschlag. available at. In: Brasseur, G.P., Jacob, D., Schuck-Zöller, S. (Eds.), Klimawandel in Deutschland: Entwicklung,

Folgen, Risiken und Perspektiven. Springer, Berlin, Heidelberg, pp. 57–66. https://doi.org/10.1007/978-3-662-50397-3_7.
Ladson, A.R., Brown, R., Neal, B., Nathan, R., 2013. A standard approach to baseflow separation using the Lyne and Hollick filter. Australas. J. Water Resour. 17, 25–34. https://doi.org/10.7158/13241583.2013.11465417.
Lang, M., Ouarda, T.B.M.J., Bobée, B., 1999. Towards operational guidelines for over-threshold modeling. J. Hydrol. 225, 103–117. https://doi.org/10.1016/S0022-1694(99)00167-5.
Lawler, D.M., Petts, G.E., Foster, I.D.L., Harper, S., 2006. Turbidity dynamics during spring storm events in an urban headwater river system: the Upper Tame, West Midlands, UK. Sci. Total Environ. 360, 109–126. https://doi.org/10.1016/j.scitotenv.2005.08.032.
Lloyd, C.E.M., Freer, J.E., Johnes, P.J., Collins, A.L., 2016. Using hysteresis analysis of high-resolution water quality monitoring data, including uncertainty, to infer controls on nutrient and sediment transfer in catchments. Sci. Total Environ. 543, 388–404. https://doi.org/10.1016/j.scitotenv.2015.11.028.
Lyne, V., Hollick, M., 1979. Stochastic time-variable rainfall-runoff modelling. In: Proceedings of the Hydrology And Water Resources Symposium. Institution of Engineers National Conference Publication, Perth, pp. 89–92.
Maneux, E., Probst, J.L., Veyssy, E., Etcheber, H., 2001. Assessment of dam trapping efficiency from water residence time: Application to fluvial sediment transport in the Adour, Dordogne, and Garonne River Basins (France). Water Resour. Res. 37, 801–811. https://doi.org/10.1029/2000WR900195.
Marcus, W.A., 1989. Lag-time routing of suspended sediment concentrations during unsteady flow. GSA Bull. 101, 644–651. https://doi.org/10.1130/0016-7606(1989)101<0644:LTROSS>2.3.CO;2.
Meschede, M., 2018. Geologie Deutschlands: ein prozessorientierter Ansatz. In: Lehrbuch, 2. Auflage. Springer Spektrum, Berlin [Heidelberg]. https://doi.org/10.1007/978-3-662-56422-6.
Mezentsev, V., 1955. Back to the computation of total evaporation. Meteorol. Gidrol. 5, 24–26.
Misset, C., Recking, A., Legout, C., Poirel, A., Cazilhac, M., 2018. Geomorphological factors influencing hysteresis patterns between suspended load and flow rate in Alpine rivers. E3S Web Conf. 40, 04004. https://doi.org/10.1051/e3sconf/20184004004.
Montgomery, D.R., 2007. Soil erosion and agricultural sustainability. Proc. Natl. Acad. Sci. 104, 13268–13272. https://doi.org/10.1073/pnas.0611508104.
Naden, P.S., 2010. The fine-sediment cascade. In: Burt, T., Allison, R. (Eds.), Sediment Cascades. John Wiley & Sons, Ltd, Chichester, UK, pp. 271–305. https://doi.org/10.1002/9780470682876.ch10.
Nathan, R.J., McMahon, T.A., 1990. Evaluation of automated techniques for base flow and recession analyses. Water Resour. Res. 26, 1465–1473. https://doi.org/10.1029/WR026i007p01465.
Oeurng, C., Sauvage, S., Sánchez-Pérez, J.-M., 2010. Dynamics of suspended sediment transport and yield in a large agricultural catchment, southwest France. Earth Surf. Process. Landf. 35, 1289–1301. https://doi.org/10.1002/esp.1971.
Oudin, L., Hervieu, F., Michel, C., Perrin, C., Andréassian, V., Anctil, F., Loumagne, C., 2005. Which potential evapotranspiration input for a lumped rainfall–runoff model? J. Hydrol. 303, 290–306. https://doi.org/10.1016/j.jhydrol.2004.08.026.
Owens, P.N., Batalla, R.J., Collins, A.J., Gomez, B., Hicks, D.M., Horowitz, A.J., Kondolf, G.M., Marden, M., Page, M.J., Peacock, D.H., Petticrew, E.L., Salomons, W., Trustrum, N.A., 2005. Fine-grained sediment in river systems: environmental significance and management issues. River Res. Appl. 21, 693–717. https://doi.org/10.1002/rra.878.
Ozturk, U., Wendi, D., Crisologo, I., Riemer, A., Agarwal, A., Vogel, K., López-Tarazón, J. A., Korup, O., 2018. Rare flash floods and debris flows in southern Germany. Sci. Total Environ. 626, 941–952. https://doi.org/10.1016/j.scitotenv.2018.01.172.
Panagos, P., Ballabio, C., Meusburger, K., Spinoni, J., Alewell, C., Borrelli, P., 2017. Towards estimates of future rainfall erosivity in Europe based on REDES and WorldClim datasets. J. Hydrol. 548, 251–262. https://doi.org/10.1016/j.jhydrol.2017.03.006.
Pelletier, A., Andréassian, V., 2020. Hydrograph separation: an impartial parametrisation for an imperfect method. Hydrol. Earth Syst. Sci. 24, 1171–1187. https://doi.org/10.5194/hess-24-1171-2020.
Rauthe, M., Steiner, H., Riediger, U., Mazurkiewicz, A., Gratzki, A., 2013. A central European precipitation climatology - part I: generation and validation of a high-resolution gridded daily data set (HYRAS). Meteorol. Z. 22, 235–256. https://doi.org/10.1127/0941-2948/2013/0436.
Schaller, M., von Blanckenburg, F., Hovius, N., Kubik, P.W., 2001. Large-scale erosion rates from in situ-produced cosmogenic nuclides in European river sediments. Earth Planet. Sci. Lett. 188, 441–458. https://doi.org/10.1016/S0012-821X(01)00320-X.
Seeger, M., Errea, M.-P., Beguería, S., Arnáez, J., Martí, C., García-Ruiz, J.M., 2004. Catchment soil moisture and rainfall characteristics as determinant factors for discharge/suspended sediment hysteretic loops in a small headwater catchment in the Spanish pyrenees. J. Hydrol. 288, 299–311. https://doi.org/10.1016/j.jhydrol.2003.10.012.
Seidel, J., Mäckel, R., 2007. Holocene sediment budgets in two river catchments in the Southern Upper Rhine Valley, Germany. Geomorphology 92, 198–207. https://doi.org/10.1016/j.geomorph.2006.07.041.
Seidel, J., Dostal, P., Imbery, F., 2012. Analysis of historical river floods - a contribution towards modern flood risk management. In: Emblemsvg, J. (Ed.), Risk Management for the Future - Theory And Cases. InTech. https://doi.org/10.5772/32463.
Skarbøvik, E., Stålnacke, P., Bogen, J., Bønsnes, T.E., 2012. Impact of sampling frequency on mean concentrations and estimated loads of suspended sediment in a Norwegian river: implications for water management. Sci. Total Environ. 433, 462–471. https://doi.org/10.1016/j.scitotenv.2012.06.072.
Skaugen, T., Onof, C., 2014. A rainfall-runoff model parameterized from GIS and runoff data. Hydrol. Process. 28, 4529–4542. https://doi.org/10.1002/hyp.9968.
Smakhtin, V.U., 2001. Low flow hydrology: a review. J. Hydrol. 240, 147–186. https://doi.org/10.1016/S0022-1694(00)00340-1.
Speckhann, G.A., Kreibich, H., Merz, B., 2021. Inventory of dams in Germany. Earth Syst. Sci. Data 13, 731–740. https://doi.org/10.5194/essd-13-731-2021.
Sun, L., Yan, M., Cai, Q., Fang, H., 2016. Suspended sediment dynamics at different time scales in the Loushui River, south-central China. Catena 136, 152–161. https://doi.org/10.1016/j.catena.2015.02.014.
Syvitski, J.P.M., Milliman, J.D., 2007. Geology, geography, and humans battle for dominance over the delivery of fluvial sediment to the coastal ocean. J. Geol. 115, 1–19. https://doi.org/10.1086/509246.
Taylor, K.G., Owens, P.N., 2009. Sediments in urban river basins: a review of sediment–contaminant dynamics in an environmental system conditioned by human activities. J. Soils Sediments 9, 281–303. https://doi.org/10.1007/s11368-009-0103-z.
Tena, A., Vericat, D., Batalla, R.J., 2014. Suspended sediment dynamics during flushing flows in a large impounded river (the lower River Ebro). J. Soils Sediments 14, 2057–2069. https://doi.org/10.1007/s11368-014-0987-0.
Tockner, K., Tonolla, D., Uehlinger, U., Siber, R., Robinson, C.T., Peter, F.D., 2009. Introduction to European rivers. In: Rivers of Europe. Elsevier, pp. 1–21. https://doi.org/10.1016/B978-0-12-369449-2.00001-1.
Turc, L., 1954. The water balance of soils: relationship between precipitations, evaporation and flow (in French: Le bilan d'eau des sols: relation entre les précipitations, l'évaporation et l'écoulement). Ann. Agron. Sér. A IV, 491–595.
Vanmaercke, M., Poesen, J., Verstraeten, G., de Vente, J., Ocakoglu, F., 2011. Sediment yield in Europe: spatial patterns and scale dependency. Geomorphology 130, 142–161. https://doi.org/10.1016/j.geomorph.2011.03.010.
Vanmaercke, M., Poesen, J., Govers, G., Verstraeten, G., 2015. Quantifying human impacts on catchment sediment yield: a continental approach. Glob. Planet. Chang. 130, 22–36. https://doi.org/10.1016/j.gloplacha.2015.04.001.
Vercruysse, K., Grabowski, R.C., 2019. Temporal variation in suspended sediment transport: linking sediment sources and hydro-meteorological drivers. Earth Surf. Process. Landf. 44, 2587–2599. https://doi.org/10.1002/esp.4682.
Vercruysse, K., Grabowski, R.C., Rickson, R.J., 2017. Suspended sediment transport dynamics in rivers: multi-scale drivers of temporal variation. Earth Sci. Rev. 166, 38–52. https://doi.org/10.1016/j.earscirev.2016.12.016.
Vercruysse, K., Grabowski, R.C., Hess, T., Lexartza-Artza, I., 2020. Linking temporal scales of suspended sediment transport in rivers: towards improving transferability of prediction. J. Soils Sediments 20, 4144–4159. https://doi.org/10.1007/s11368-020-02673-5.
Walling, D.E., 1983. The sediment delivery problem. J. Hydrol. 65, 209–237. https://doi.org/10.1016/0022-1694(83)90217-2.
Walling, D.E., 2006. Human impact on land-ocean sediment transfer by the world's rivers. Geomorphology 79, 192–216. https://doi.org/10.1016/j.geomorph.2006.06.019.
Walling, D.E., Fang, D., 2003. Recent trends in the suspended sediment loads of the world's rivers. Glob. Planet. Chang. 39, 111–126. https://doi.org/10.1016/S0921-8181(03)00020-1.
Walling, D., Webb, W., 1981. The reliability of suspended sediment load data. In: Erosion And Sediment Transport Measurement (Proceedings of the Florence Symposium). IAHS Publication, pp. 177–194.
Warrick, J.A., 2015. Trend analyses with river sediment rating curves. Hydrol. Process. 29, 936–949. https://doi.org/10.1002/hyp.10198.
Wohl, E., 2015. Legacy effects on sediments in river corridors. Earth Sci. Rev. 147, 30–53. https://doi.org/10.1016/j.earscirev.2015.05.001.
WSV (Wasserstraßen- und Schifffahrtsverwaltung des Bundes), 2022. Digitale Bundeswasserstraßenkarte. available at. https://www.gdws.wsv.bund.de/SharedDocs/Downloads/DE/Karten/Karten_neu/DBWK1000_Generaldirektion.html.
Zeder, J., Fischer, E.M., 2020. Observed extreme precipitation trends and scaling in Central Europe. WeatherClim.Extr. 29, 100266 https://doi.org/10.1016/j.wace.2020.100266.